

Polyoxoanion-Supported Organometallic Complexes: Carbonyls of Rhenium(I), Iridium(I), and Rhodium(I) That Are Soluble Analogs of Solid-Oxide-Supported $M(\text{CO})_n^+$ and That Exhibit Novel $M(\text{CO})_n^+$ Mobility

Toshi Nagata,^{1a,b} Matthias Pohl,^{1a} Heiko Weiner,^{1a,c} and Richard G. Finke*,^{1a}

Department of Chemistry, Colorado State University, Fort Collins, Colorado 80523

Received August 1, 1996[⊗]

The Dawson-type $\text{P}_2\text{W}_{15}\text{Nb}_3\text{O}_{62}^{9-}$ polyoxoanion-supported $\text{Re}(\text{CO})_3^+$ complex, $[\text{Re}(\text{CO})_3 \cdot \text{P}_2\text{W}_{15}\text{Nb}_3\text{O}_{62}]^{8-}$ (**1**), has been synthesized and characterized in two different counter-cation compositions. The $[(n\text{-C}_4\text{H}_9)_4\text{N}]_8^{8+}$ complex provides a highly soluble compound which exists as a single isomer in solution. The carbonyl stretching infrared frequencies suggest that the $\text{P}_2\text{W}_{15}\text{Nb}_3\text{O}_{62}^{9-}$ ligand serves as a strong electron donor to the $\text{Re}(\text{CO})_3^+$ fragment. The $\text{P}_2\text{W}_{15}\text{Nb}_3\text{O}_{62}^{9-}$ polyoxoanion-supported $\text{Ir}(\text{CO})_2^+$ complex $[\text{Ir}(\text{CO})_2 \cdot \text{P}_2\text{W}_{15}\text{Nb}_3\text{O}_{62}]^{8-}$ (**2**) has also been synthesized and characterized as its octakis(tetrabutylammonium), $[(n\text{-C}_4\text{H}_9)_4\text{N}]_8^{8+}$, salt. This compound was characterized by NMR and IR, results which demonstrate that **2** also exists as a single isomer in solution. The $[\text{Ir}(\text{CO})_2 \cdot \text{P}_2\text{W}_{15}\text{Nb}_3\text{O}_{62}]^{8-}$ complex is stable in the absence of water, but decomposes quickly in the presence of even 1 equiv of water. Attempted preparation of the analogous $\text{P}_2\text{W}_{15}\text{Nb}_3\text{O}_{62}^{9-}$ -supported $\text{Rh}(\text{CO})_2^+$ complex (**3**), while monitoring by ^{31}P NMR, revealed that this compound is unstable in solution at room temperature. In addition, we have discovered that added Na^+ can induce the formation of non- C_{3v} symmetry isomers of supported $\text{Re}(\text{CO})_3^+$ and $\text{Ir}(\text{CO})_2^+$ and, by inference, supported $\text{Ir}(1,5\text{-COD})^+$. When Na^+ is removed from these systems by addition of Kryptofix[2.2.2], the non- C_{3v} isomers convert back to the single, C_{3v} isomer with heating, thereby providing a model system for the little studied mobility of $M(\text{CO})_n^+$ cations across a soluble-oxide surface. When $[\text{Rh}(\text{CO})_2 \cdot \text{P}_2\text{W}_{15}\text{Nb}_3\text{O}_{62}]^{8-}$ is irradiated in the presence of hydrogen and cyclohexene a novel polyoxoanion-stabilized Rh^0_n nanocluster is formed, results that bear a strong analogy to Yates' work studying atomically-dispersed $\text{Rh}(\text{CO})_2^+$ on solid Al_2O_3 .^{10e} Yates and co-workers observe that $\text{Rh}(\text{CO})^+ \cdot \text{Al}_2\text{O}_3$ loses a CO upon photolysis, and that the resultant $\text{Rh}(\text{CO})_1^+ \cdot \text{Al}_2\text{O}_3$ is reduced under H_2 to form $\text{Rh}(0)$, which in turn yields Rh^0_n clusters on Al_2O_3 —a process that, intriguingly, is largely reversible if CO is readded. Also briefly discussed is other relevant literature of solid-oxide-supported $\text{Re}(\text{CO})_3^+$ and $M(\text{CO})_2^+$ ($M = \text{Ir}, \text{Rh}$), literature that makes apparent the potential significance of these complexes as EXAFS and other spectroscopic models of solid-oxide-supported $M(\text{CO})_n^+$.

Introduction

Metal carbonyl complexes supported on the metal–oxide surface have been the focus of numerous studies.² Interest in these systems stems from the fact that metal carbonyls supported on solid oxides are among the best studied probes of the difficult to study, and thus poorly understood, oxide-to-metal catalyst-support interaction. Particularly well-studied systems are $\text{Rh}(\text{CO})_2^+$ on Al_2O_3 ^{3–6} and on other metal oxides^{7,8} and $\text{Re}(\text{CO})_3^+$ on MgO ⁹ for which the structures shown in Figure 1 have been proposed. Arguably, these structures are better characterized than any other oxide-supported complexes in heterogeneous

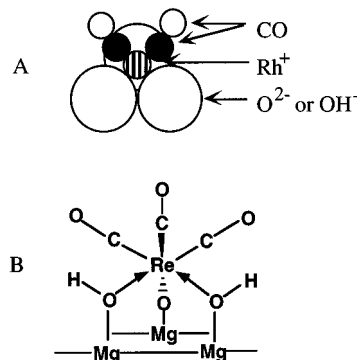


Figure 1. (A) Proposed structure of Rh^{I} geminal dicarbonyl sites on $\gamma\text{-Al}_2\text{O}_3$, $[\text{Rh}(\text{CO})_2]^+ \cdot \text{Al}_2\text{O}_3$, suggested by van't Blik et al.⁴ Note that the five-coordinate $\text{Rh}^{\text{I}}(\text{CO})_2^+$ species in Figure 1A is not what a considerable amount of organometallic precedent suggests (see the references, and a more general discussion of the factors for or against five coordination in nominally four-coordinate, d^8 complexes, provided elsewhere,^{16j} especially footnotes 15, 26, and 30 therein^{16j}). (B) Proposed structure of the rhenium tricarbonyl sites on magnesia, $[\text{Re}(\text{CO})_3]^+ \cdot \text{MgO}$.^{9a}

catalysis, although their structures are still not unequivocally established at the atomic level. More recently, photochemical activation of hydrocarbons by Al_2O_3 -supported rhodium car-

[⊗] Abstract published in *Advance ACS Abstracts*, February 15, 1997.

- (1) (a) Colorado State University, Fort Collins, Colorado, 80523. (b) Permanent address: Department of Chemistry, Graduate School of Science, Kyoto University, Kyoto 606-01, Japan. (c) Permanent address: Department of Chemistry, TU Bergakademie Freiberg, D-09596 Freiberg, Germany.
- (2) Reviews: (a) Gates, B. C. *Chem. Rev.* **1995**, *95*, 511. (b) Lamb, H. H.; Gates, B. C.; Knözinger, H. *Angew. Chem., Int. Ed. Engl.* **1988**, *27*, 1127.
- (3) Yang, A. C.; Garland, C. W. *J. Phys. Chem.* **1957**, *61*, 1504.
- (4) van't Blik, H. F. J.; van Zon, J. B. A. D.; Huizinga, T.; Vis, J. C.; Koningsberger, D. C.; Prins, R. *J. Am. Chem. Soc.* **1985**, *107*, 3139.
- (5) Frederick, B. G.; Apai, G.; Rhodin, T. N. *J. Am. Chem. Soc.* **1987**, *109*, 4797.
- (6) Binsted, N.; Evans, J.; Greaves, G. N.; Price, R. J. *Organometallics* **1989**, *8*, 613.
- (7) Herrero, J.; Blanco, C.; González-Elipse, A. R.; Espinós, J. P.; Oro, L. A. *J. Mol. Catal.* **1990**, *62*, 171.
- (8) Buchanan, D. A.; Hernandez, E.; Solymosi, F.; White, J. M. *J. Catal.* **1990**, *125*, 456.

- (9) (a) Kirilin, P. S.; DeThomas, F. A.; Bailey, J. W.; Gold, H. S.; Dybowski, C.; Gates, B. C. *J. Phys. Chem.* **1986**, *90*, 4882. (b) Fung, A. S.; Tooley, P. A.; Kelley, M. J.; Koningsberger, D. C.; Gates, B. C. *J. Phys. Chem.* **1991**, *95*, 225.

bonyls that agglomerate, under H_2 , to Rh^0_n particles has been reported,¹⁰ work which further illustrates the interest in well-characterized, oxide-supported $M(CO)_x^+$ species.

The available solid-oxide-supported metal carbonyls have been studied by multiple physical techniques, the most powerful being EXAFS (extended X-ray absorption fine structure).¹¹ EXAFS can provide bond lengths, numbers and types of neighboring atoms, and deviations of atoms from equilibrium position, as well as short-range order and local structure around particular atoms. However, in order to unequivocally interpret EXAFS spectra without error, discrete model or reference compounds are well-known to be invaluable. For the $M(CO)_x^+$ -solid-oxide systems, the ideal model complexes—which are not presently available—should have the following properties: (i) a stoichiometrically well-defined, preferably 1:1, ratio of metal to support, (ii) a nonaggregated, monomeric form, (iii) existence as a single isomer, (iv) solubility in a variety of solvents, thereby facilitating solution structure determinations, and, ideally as well, (v) sufficient crystallinity to permit single-crystal X-ray diffraction structural determinations.

Polyoxoanion-supported $M(CO)_n^+$ are promising candidates for modeling solid-oxide-supported metal carbonyls, in light of the close-packed oxide nature of both solid metal oxides and polyoxoanions.^{12,13} In addition, a few polyoxoanion-supported metal carbonyls have already been described in the literature,^{14,15} although the only—but still major—contributions to date were made by Klemperer, Day, and co-workers. Specifically, these

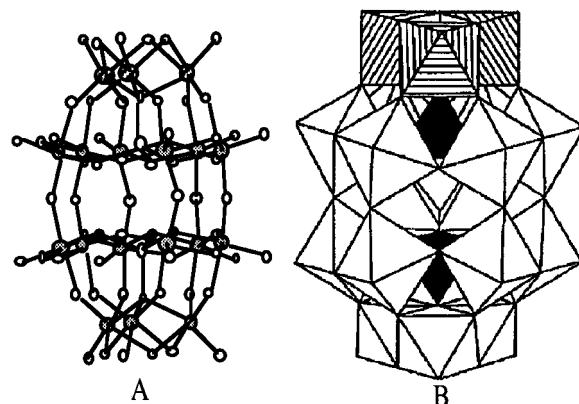


Figure 2. (A) Ball-and-stick representation of α -1,2,3- $P_2W_{15}Nb_3O_{62}^{9-}$ as determined by a single crystal X-ray diffraction structural analysis.^{16c} (B) Polyhedral representation of α -1,2,3- $P_2W_{15}Nb_3O_{62}^{9-}$. The three NbO_6 octahedra are represented by the hatched octahedra in the top 1, 2, and 3 positions. The WO_6 octahedra occupy positions 4–18 (the white octahedra), and the PO_4 groups are shown as the two internal black tetrahedra.

authors have reported the first and still only examples of polyoxoanion-supported manganese and rhenium complexes^{14a,b} ($[Mn(CO)_3 \cdot (cis-Nb_2W_4O_{19})]^{3-}$ and $[Re(CO)_3 \cdot (cis-Nb_4W_4O_{19})]^{3-}$), as well as the first examples of iridium and rhodium carbonyl complexes,^{14d} $\{[Rh(CO)_2]_5(Nb_2W_4O_{19})_2\}^{3-}$, $\{[Rh(CO)_2]_3(Nb_2W_4O_{19})_2\}^{5-}$, and $\{[Ir(CO)_2]_2H(Nb_2W_4O_{19})_2\}^{5-}$. Unfortunately, however, the complexes of $Mn(CO)_3^+$ and $Re(CO)_3^+$, are a mixture of three diastereomers, and both the iridium and the rhodium dicarbonyls exhibit metal to polyoxoanion stoichiometries other than the desired 1:1 ratio. These two facts preclude the use of the $cis-Nb_2W_4O_{19}^{4-}$ -supported compounds as soluble EXAFS models; the multiple support sites, and lower, non- C_{3v} symmetry of the most basic support site in $cis-Nb_2W_4O_{19}^{4-}$ are other nonoptimum features of this early system.

The trimetaphosphate-supported metal carbonyls, $[Mn(CO)_3 \cdot (P_3O_9)]^{2-}$, $[Re(CO)_3 \cdot (P_3O_9)]^{2-}$, and $[Ir(CO)_2 \cdot (P_3O_9)]^{2-}$ have also been reported by Klemperer, Day, and co-workers,^{14c,d} and these complexes do exist as single isomers in solution. In addition, they are also generally characterized by X-ray diffraction structural analyses, key results underpinning the development of polyoxoanion-supported metal carbonyls. They are, therefore, of (unexploited) interest as EXAFS models, their main limitation being that the trimetaphosphate support does not, of course, contain metal atoms and thus is not, strictly speaking, rigorously analogous to a transition-metal oxide.

For some time now we have had studies in progress aimed at well characterized, single isomer, 1:1 metal–polyoxoanion complexes of metal carbonyl complexes. Our choice of $P_2W_{15}Nb_3O_{62}^{9-}$, Figure 2, as the support system was prompted by its now well-documented tendency to form nonaggregated, 1:1 polyoxoanion to metal, single isomer adducts,¹⁶ as has been demonstrated for $[Ir(1,5-COD) \cdot P_2W_{15}Nb_3O_{62}]^{8-}$ by ¹⁷O and ¹⁸³W NMR studies^{16g,j} and for $[Rh(C_5Me_5) \cdot P_2W_{15}Nb_3O_{62}]^{7-}$ by single-crystal X-ray crystallography and ¹⁸³W NMR.¹⁶ⁱ The $P_2W_{15}Nb_3O_{62}^{9-}$ -based system is, therefore, as good a soluble-oxide systems as is presently available for preparing EXAFS

- (10) (a) Yates, J. T., Jr.; Duncan, T. M.; Worley, S. D.; Vaghan, R. W. *J. Chem. Phys.* **1979**, *70*, 1219. (b) Basu, P.; Panayotov, D.; Yates, J. T., Jr. *J. Am. Chem. Soc.* **1988**, *110*, 2074. (c) Ballinger, T. H.; Yates, J. T., Jr. *J. Am. Chem. Soc.* **1992**, *114*, 10074. (d) Wong, J. C. S.; Yates, J. T., Jr. *J. Am. Chem. Soc.* **1994**, *116*, 1610. (e) Wovchko, E. A.; Yates, J. T., Jr. *J. Am. Chem. Soc.* **1995**, *117*, 12557.
- (11) See, for example: Koningsberger, D. C.; Prins, R. *Trends Anal. Chem.* **1981**, *1*, 16. Teo, B. K.; Joy, D. C., Eds. *EXAFS Spectroscopic Techniques and Applications*; New York: Plenum, 1981.
- (12) Polyoxoanion lead references: (a) Pope, M. T. *Heteropoly and Isopoly Oxometalates*; Springer-Verlag: New York, 1983. (b) *Polyoxometalates: From Platonic Solids to Anti-Retroviral Activity*; Proceedings of the July 15–17, 1992, Meeting at the Center for Interdisciplinary Research in Bielefeld, Germany; Müller, A.; Pope, M. T., Eds.; Kluwer Publishers: Dordrecht, The Netherlands, 1992.
- (13) (a) The resemblance of polyoxoanions to discrete fragments of solid-metal oxides was first noted by Professor Baker: Baker, L. C. W. In *Advances in the Chemistry of Coordination Compounds*; Kirschner, S., Ed.; Macmillan: New York, 1961; p 604. (b) For a more exact analogy, see elsewhere^{13c} where the structural similarity between a hypothetical $[PW_9O_{34}(ZnO_3)]^{9-}$ and the (0001) surface of ZnO is briefly discussed. Also, the 4-fold symmetry “ W_4O_8 ” site on the surface anions such as in the “belt” region of the Wells–Dawson $P_2W_{18}O_{62}^{6-}$ anion bears an obvious visual resemblance to the (100) surface of monoclinic WO_3 .^{13d,e} (c) Finke, R. G.; Droegge, M.; Hutchinson, J. R.; Gansow, O. *J. Am. Chem. Soc.* **1981**, *103*, 1587. (d) Figueras, F.; Figlarz, M.; Portezax, J. L.; Forissier, M.; Gerand, B.; Guenet, J. J. *Catal.* **1981**, *71*, 389. (e) WO_3 has essentially the ReO_3 perovskite structure: Wells, A. F. *Structural Inorganic Chemistry*; Clarendon Press: Oxford, U.K., 1995; pp 173, 474. (f) For our preliminary studies of $[Rh(1,5-COD) \cdot P_2W_{15}Nb_3O_{62}]^{8-}$, its conversion under CO to $[Rh(CO)_2 \cdot P_2W_{15}Nb_3O_{62}]^{8-}$, and the ability of these catalyst precursors to yield what we now know are polyoxoanion-stabilized, Rh^0_{xx} nanocluster catalysts,²⁷ see: Edlund, D. J. Ph. D. Dissertation, University of Oregon, 1987. Complete studies of the synthesis, characterization and catalytic reactivity of polyoxoanion-stabilized Rh_{xx} nanoclusters, generated by hydrogenation of pure, well-characterized $[Rh(1,5-COD) \cdot P_2W_{15}Nb_3O_{62}]^{8-}$, have been in progress for some time now, and will be reported in due course (Aiken, J.; Weddle, K.; Edlund, D. J.; Finke, R. G. Unpublished results and experiments in progress).
- (14) (a) Besecker, C. J.; Klemperer, W. G. *J. Am. Chem. Soc.* **1980**, *102*, 7598. (b) Besecker, C. J.; Day, V. W.; Klemperer, W. G.; Thompson, M. R. *Inorg. Chem.* **1985**, *24*, 44. (c) Besecker, C. J.; Day, V. W.; Klemperer, W. G. *Organometallics* **1985**, *4*, 564. (d) Klemperer, W. G.; Main, D. J. *Inorg. Chem.* **1990**, *29*, 2355. (e) Besecker, C. J.; Day, V. W.; Klemperer, W. G.; Thompson, M. R. *J. Am. Chem. Soc.* **1984**, *106*, 4125. (f) Day, V. W.; Klemperer, W. G.; Main, D. J. *Inorg. Chem.* **1990**, *29*, 2345.

- (15) (a) The solid-state reaction chemistry of nonbasic polyoxoanions (*i.e.* $SiW_{12}O_{40}^{4-}$, $SiMo_{12}O_{40}^{3-}$, $PW_{12}O_{40}^{3-}$, $PMo_{12}O_{40}^{3-}$ [$x = 3$ and 4], and $PVMo_{11}O_{40}^{4-}$) and bis(triphenylphosphine)rhodium(I) carbonyl derivatives has been reported.^{15b} These, however, are not polyoxoanion-supported complexes; indeed, direct evidence available as part of Siedle and co-workers’ studies demonstrated that the Rh(I) center and these non-basic polyoxoanions are too far apart for any direct interaction. (b) Siedle, A. R.; Gleason, W. B.; Newmark, R. A.; Skarjune, R. P.; Lyon, P. A.; Markell, C. G.; Hodgson, K. O.; Roe, A. L. *Inorg. Chem.* **1990**, *29*, 1667.

and related spectroscopic models. Also of significance is that $P_2W_{15}Nb_3O_{62}^{9-}$ is the only polyoxometalate to date which offers a C_{3v} symmetry (“ $Nb_3O_9^{3-}$ ”) support site to begin to test, in a soluble and thus more readily and fully characterizable system, the proposed, EXAFS-derived structures shown back in Figure 1, structures that involve a C_{3v} symmetry site within the solid oxide. The one, main limitation of larger, more highly charged systems such as $P_2W_{15}Nb_3O_{62}^{9-}$ derives from the difficulties in obtaining good, strongly diffracting, single crystals of such high-charge polyoxoanions soluble in (and thus recrystallized from) non-aqueous solutions. Preliminary work was initiated more than a decade ago, with “[$Rh(CO)_2 \cdot P_2W_{15}Nb_3O_{62}$] $^{8-}$ ” being reported in a Ph.D. thesis in 1987,^{13f} but we were never satisfied with the synthesis, characterization, or stability of that particular material.

Herein we report the culmination of our efforts on the synthesis, isolation, and spectroscopic characterization of the $P_2W_{15}Nb_3O_{62}^{9-}$ -supported $Re(CO)_3^+$ and $Ir(CO)_2^+$ complexes, [$Re(CO)_3 \cdot P_2W_{15}Nb_3O_{62}$] $^{8-}$ (1) and [$Ir(CO)_2 \cdot P_2W_{15}Nb_3O_{62}$] $^{8-}$ (2), as their [$(n-C_4H_9)_4N$] $^+$ or mixed [$(n-C_4H_9)_4N$] $^+$ and Na^+ salts. Our attempted synthesis of clean, single-isomer complexes of $Rh(CO)_2^+$, [$Rh(CO)_2 \cdot P_2W_{15}Nb_3O_{62}$] $^{8-}$ (3), is also reported, work that unequivocally demonstrates the instability of the $Rh(CO)_2^+$ complex in solution at room temperature. Of perhaps special interest is our discovery that new, lower symmetry, isomers of $Re(CO)_3^+$, $Ir(CO)_2^+$ (and, by inference, $Ir(1,5-COD)^+$) can be induced by added Na^+ cation. The resulting systems revert to the thermodynamically more stable isomers with heating, thereby providing heretofore unavailable model systems for future studies of $M(CO)_n^+$ mobility across a soluble-oxide surface.

Experimental Section

Materials. The following compounds were obtained from the manufacturer, stored in the drybox, and used without further purification: $AgBF_4$, [$Ir(1,5-COD)Cl$] $_2$, [$Rh(1,5-COD)Cl$] $_2$, $Re_2(CO)_{10}$ (Strem); acetonitrile, ethyl acetate, diethyl ether (all HPLC grade), 4,7,13,16-, 21,24-hexaoxa-1,10-diazabicyclo[8.8.8]hexacosane [Kryptofix[2.2.2.]] (Aldrich); CD_3CN , CD_2Cl_2 (Isotec). Methylene chloride (Fisher, ACS grade) was treated with concentrated sulfuric acid to remove cyclohexene stabilizer, and then distilled from CaH_2 under argon. Carbon monoxide (Matheson, 99.5% purity) was purified by passing it through a disposable oxygen trap (200 cm^3 ; Baxter G5301-2) and a disposable moisture trap (Molecular Sieves 13X + 4Å, 75 cm^3 ; Baxter G5301-12). Argon was purchased from General Air and purified by passing through a reduced R3-11 catalyst (BASF) and 4 Å molecular sieves (Linde).

[$(n-C_4H_9)_4N$] $_9P_2W_{15}Nb_3O_{62}$ was prepared by our most recent procedure,¹⁷ an improved version of our original synthesis.¹⁶ⁱ $Re(CO)_5Br$

was prepared from $Re_2(CO)_{10}$ according to the literature procedures.¹⁸ [$Re(CO)_3(CH_3CN)_3$] BF_4 ¹⁹ was prepared from $Re(CO)_5Br$ according to the procedures described for the preparation of the analogous ClO_4^- salt,^{19a} but using $AgBF_4$ instead of $AgClO_4$.

Instrumentation/Analytical Procedures. Oxygen- and moisture-sensitive samples were routinely manipulated under an inert nitrogen atmosphere in a Vacuum Atmospheres drybox (≤ 1 ppm oxygen as monitored by use of a Vacuum Atmospheres oxygen monitor, VAC Model AO 316-C). All glassware used in the drybox was dried overnight at 120 °C before use. Elemental analyses were obtained from Mikroanalytisches Labor Pascher, Remagen, Germany. Infrared spectra were obtained on a Nicolet 5DX spectrometer as either KBr discs or as solutions (CH_3CN) using a NaCl cell (pathlength 0.1 mm). KBr (Aldrich, spectrophotometric grade) was used as received.

Gas uptake experiments were conducted using standard technique with a mercury manometer and a vacuum line.²⁰ The total volume of the system was 111 ± 1 cm^3 as measured by the pressure change induced by opening the stopcock of a standard calibrated flask (28.6 cm^3). The uptake of gas was quantitatively determined by monitoring the pressure decrease with a manometer (± 1 Torr; 1 Torr = 133.32 Pa; detailed procedures are available as Supporting Information). Control experiments showed a negligible uptake (< 1 Torr) in the absence of [$M(1,5-COD) \cdot P_2W_{15}Nb_3O_{62}$] $^{8-}$ ($M = Ir, Rh$) compound, thereby confirming the absence of leaks or other artifacts in the gas uptake experiments.

Gas-liquid chromatographic (GC) monitoring of the amount of 1,5-cyclooctadiene released from such CO uptake experiments was done using a Hewlett-Packard 5890 Series II gas chromatograph equipped with a HP 3395 integrator. A DB-1 capillary column was used under the following conditions: initial temperature 50 °C, initial time 3 min, temperature ramp 10 °C/min, final temperature 160 °C, injector temperature 180 °C, detector (FID) temperature 200 °C, He carrier gas flow 1.5–2 cm^3/min , and sample volume 2 μL . Toluene was used as an internal standard.

Nuclear Magnetic Resonance (NMR). All NMR spectra were obtained in Wilmad NMR tubes (5 mm or 10 mm o.d.) equipped with a J. Young valve, at room temperature unless otherwise stated. The chemical shifts are reported on the δ scale with downfield resonances as positive.

³¹P NMR (121.5 MHz) spectra were recorded in 5 mm o.d. tubes on a Bruker AC-300P NMR spectrometer. A 33 mM CD_3CN solution (0.020 mmol of polyoxoanion in 0.6 mL) was used unless otherwise stated. An external reference of 85% H_3PO_4 was used by the substitution method.²¹ Acquisition parameters are as follows: pulse width 5 μs , acquisition time 0.819 s, relaxation delay 1.500 s, and sweep width ± 10000 Hz. An exponential line broadening apodization (1.5 Hz) was applied to all spectra, but removed for any line widths reported herein.

¹⁹F NMR (282.4 MHz) spectra were also recorded in 5 mm o.d. tubes on a Bruker AC-300P NMR spectrometer. In all measurements, we used a CD_3CN solution containing 33 mM of polyoxoanion and 28 mM (0.85 equiv) of $(n-C_4H_9)_4NPF_6$. The PF_6^- resonance ($\delta = -72.3$

(16) Earlier Oregon work focused toward $P_2W_{15}Nb_3O_{62}^{9-}$ -based polyoxoanion-supported complexes: (a) Edlund, D. J.; Saxton, R. J.; Lyon, D. K.; Finke, R. G. *Organometallics* **1988**, *7*, 1692. (b) Nomiyama, K.; Pohl, M.; Mizuno, N.; Lyon, D. K.; Finke, R. G. *Inorg. Synth.* **1997**, *31*, 186. (c) Finke, R. G.; Nomiyama, K.; Green, C. A.; Droegge, M. W.; *Inorg. Synth.* **1992**, *29*, 239. (d) Finke, R. G.; Lyon, D. K.; Nomiyama, K.; Sur, S.; Mizuno, N. *Inorg. Chem.* **1990**, *29*, 1784–1787, 1787–1789. (e) Finke, R. G.; Lyon, D. K.; Nomiyama, K.; Weakley, T. J. R. *Acta Crystallogr.* **1990**, *C46*, 1592. (f) Trovarelli, A.; Finke, R. G. *Inorg. Chem.* **1993**, *32*, 6034. (g) Pohl, M.; Finke, R. G. *Organometallics* **1993**, *12*, 1453. (h) Nomiyama, K.; Kaneko, M.; Kasuga, N.; Finke, R. G.; Pohl, M. *Inorg. Chem.* **1994**, *33*, 1469. (i) Pohl, M.; Lin, Y.; Weakley, T. J. R.; Nomiyama, K.; Kaneko, M.; Finke, R. G. *Inorg. Chem.* **1995**, *34*, 767. (j) Pohl, M.; Lyon, D. K.; Mizuno, N.; Nomiyama, K.; Finke, R. G. *Inorg. Chem.* **1995**, *34*, 1413. (k) Nomiyama, K.; Nozaki, C.; Kaneko, M.; Finke, R. G.; Pohl, M. *J. Organomet. Chem.* **1995**, *505*, 23. (l) Work on $P_2W_{15}Nb_3O_{62}^{9-}$ polyoxoanion-stabilized Ir^{0-300} and Ir^{0-900} nanoclusters: Lin, Y.; Finke, R. G. *J. Am. Chem. Soc.* **1994**, *116*, 8335. Lin, Y.; Finke, R. G. *Inorg. Chem.* **1994**, *33*, 4891. (m) C_3 symmetry is seen for the $CpTi^{3+}$ supported upon the vanadium analog, $P_2W_{15}V_3O_{62}^{9-}$: Rapko, B. M.; Pohl, M.; Finke, R. G. *Inorg. Chem.* **1994**, *33*, 3624.

(17) Weiner, H.; Aiken, J. D. III; Finke, R. G. *Inorg. Chem.* **1996**, *35*, 7905.

(18) Schmidt, S. P.; Trogler, W. C.; Basolo, F. *Inorg. Synth.* **1990**, *28*, 162.

(19) (a) Edwards, D. A.; Marshalsea, J. J. *Organomet. Chem.* **1977**, *131*, 73. (b) An X-ray crystal structure of [$Re(CO)_3(CH_3CN)_3$] BF_4 has been reported: Chan, L. Y. Y.; Isaacs, E. E.; Graham, W. A. G. *Can. J. Chem.* **1977**, *55*, 111.

(20) Shriver, D. F.; Drezdson, M. A. *The Manipulation of Air-Sensitive Compounds*, 2nd ed.; John Wiley & Sons: New York, 1986; pp 129–137.

(21) The reported chemical shifts are not corrected for the volume diamagnetic susceptibility of the sample's solution, but proved reproducible *in house* within ± 0.2 ppm when using the same NMR instrument, similar NMR sample tubes, and similar volumes and concentrations (as was done for all samples in the present study). Elsewhere (see especially footnotes 34 and 51),¹⁶ⁱ we have discussed the problem that literature chemical shifts variations as large as ± 0.5 ppm are not uncommon due to the solution's volume susceptibility.

(22) (a) Finke, R. G.; Nomiyama, K.; Green, C. A.; Droegge, M. W. *Inorg. Synth.* **1992**, *29*, 239. (b) Lin, Y.; Nomiyama, K.; Finke, R. G. *Inorg. Chem.* **1993**, *32*, 6040.

ppm, referenced to neat CFCl_3 by the external substitution method,²¹ doublet, $^1J(^3\text{P}^{19}\text{F}) = 706$ Hz) was used as internal standard both for chemical shifts and quantitative analysis by integration of the signals; the "number of fluorines, F" in the text that follows was calculated from the ratio of integrated intensities, assuming this -72.3 ppm signal to be 5.1 F (= 0.85 equiv of PF_6^- ; this internal standard signal is not listed among the data for each individual compound). Acquisition parameters are as follows: pulse width 3.0 μs , acquisition time 0.623 s, relaxation delay 1.500 s, and sweep width ± 13158 Hz (*i.e.*, from -63 ppm to -155 ppm). An exponential line-broadening apodization (1.5 Hz) was applied to all spectra, but was removed from any reported line widths. To ensure that the delay was long enough for the complete relaxation of all signals, a longer delay (4.500 s) was also applied in control experiments; the resultant integrated intensities of the signals were the same within experimental error ($\pm 5\%$).

¹⁸³W NMR (20.8 MHz) spectra were recorded on a Bruker AM500 NMR spectrometer. Spectra were recorded at room temperature in 10 mm o.d. NMR tubes and referenced to saturated $\text{Na}_2\text{WO}_4/\text{D}_2\text{O}$ by the external substitution method.²¹ Acquisition parameters were as follows: pulse width 30 μs , acquisition time 1.114 s, relaxation delay 1.000 s, and sweep width ± 14705 Hz. An exponential line-broadening apodization (5 Hz) was applied to all spectra, but was removed for any line widths reported herein.

Preparations. $[(n\text{-C}_4\text{H}_9)_4\text{N}]_8[\text{Re}(\text{CO})_3\cdot\text{P}_2\text{W}_{15}\text{Nb}_3\text{O}_{62}]\cdot(n\text{-C}_4\text{H}_9)_4\text{NBF}_4$, **1a**. In the drybox, $[(n\text{-C}_4\text{H}_9)_4\text{N}]_9\text{P}_2\text{W}_{15}\text{Nb}_3\text{O}_{62}$ (3.0 g, 0.48 mmol) was dissolved in 18 mL of CH_3CN . To this clear, colorless solution was added a solution of $[\text{Re}(\text{CO})_3(\text{CH}_3\text{CN})_3]\text{BF}_4$ (240 mg, 0.50 mmol, in 2 mL of CH_3CN) dropwise over 5 min. The solution color changed to green. After being stirred overnight at room temperature, the solution was evacuated to dryness at room temperature. The yellow-brown residual solid was dissolved in 3 mL of CH_3CN , and the resulting brown solution was added dropwise (over 4 min) to 200 mL of diethyl ether with vigorous stirring. A pale yellow powder formed immediately. The suspension was stirred for 30 min, and the pale yellow powder was collected on a medium frit, washed with 20 mL of ether, and dried in vacuo at room temperature overnight. Yield: 2.88 g (0.43 mmol, 91%). Anal. Calcd (found) for $\text{C}_{147}\text{H}_{324}\text{N}_9\text{ReP}_2\text{W}_{15}\text{Nb}_3\text{O}_{62}\cdot\text{BF}_4$: C, 26.63 (26.57, 26.60); H, 4.93 (5.01, 5.01); N, 1.90 (2.04, 1.99); O, 15.69 (15.2, 15.4); P, 0.93 (0.91, 0.91); Nb, 4.20 (4.26, 4.36); W, 41.60 (41.9, 42.3); Re, 2.81 (2.23, 2.25), total, 100.0 (98.1, 98.8). IR (KBr pellet, cm^{-1}): ν_{CO} 2006 (s), 1876 (s); polyoxometalate region 1083 (vs), 1060 (m), 1010 (w), 941 (s), 913 (s), 896 (s), 798 (vs). ³¹P NMR (33 mM in CD_3CN , 200 scans), δ (no. of P, $\Delta\nu_{1/2}$): -7.74 (1P, 1.8 ± 0.1 Hz), -13.36 (1P, 2.0 ± 0.1 Hz). ¹⁹F NMR (32 scans), δ (no. of F, $\Delta\nu_{1/2}$): -151.1 (4.0 F [=1.0 equiv of BF_4^-], 1.7 ± 0.1 Hz). ¹⁸³W NMR (80 mM of **1** in CD_3CN), δ (no. of W, $\Delta\nu_{1/2}$): -126 (3W, 3 ± 1 Hz), -147 (6W, 5 ± 1 Hz), -182 (6W, 3 ± 1 Hz).

Air Stability of 1a. The stability of **1a** in air was established by a comparison of ³¹P-NMR and IR spectra of a freshly prepared 33 mM solution of **1a**, in CD_3CN in a J. Young NMR tube first before, and then after, exposure to air for 2 weeks, without protection from diffuse room light. No significant differences between the two were observed, establishing the stability of **1a** to air for ≥ 2 weeks and to the diffuse light and other stated conditions of this control experiment.

Attempted Removal of $(n\text{-C}_4\text{H}_9)_4\text{NBF}_4$ from 1a by Its Re-precipitation. From $\text{CH}_3\text{CN}/\text{EtOAc}$. The compound **1a** (1.7 g, 0.25 mmol) was dissolved in 3 mL of CH_3CN . To this solution was added 150 mL of ethyl acetate in 25 mL portions. After addition of 100 mL, a small amount of unidentified brown precipitate formed, which was removed by filtration. After complete addition of the 150 mL of ethyl acetate, the solution was clear yellow. Addition of ether (100 mL) to this solution gave a yellow precipitate of **1a**, which was collected by filtration, washed with ether, and dried in vacuum overnight (0.97 g, 0.15 mmol, 57%). ¹⁹F NMR of this material confirmed that 1.0 equiv of $(n\text{-C}_4\text{H}_9)_4\text{NBF}_4$ was still present.

From $\text{CH}_2\text{Cl}_2/\text{EtOAc}$. The compound **1a** (700 mg, 0.11 mmol) was dissolved in 0.4 mL of CH_2Cl_2 . To this clear yellow solution was added ethyl acetate (0.8 mL). A small amount of an unidentified pale yellow precipitate formed, which was removed by filtration through a membrane filter (Gelman Acrodisc 13CR, PTFE 0.2 μm). The clear yellow filtrate was kept at -20 °C for 48 h, to give yellow microcrystals. These microcrystals were collected on a filter frit,

washed with ether, and dried in vacuo overnight (153 mg, 0.023 mmol, 22%). ¹⁹F NMR of this material showed the presence of 0.83 equiv of $(n\text{-C}_4\text{H}_9)_4\text{NBF}_4$, that is, only 0.17 equiv of this contaminant was removed by this procedure.

$[(n\text{-C}_4\text{H}_9)_4\text{N}]_5\text{Na}_3[\text{Re}(\text{CO})_3\cdot\text{P}_2\text{W}_{15}\text{Nb}_3\text{O}_{62}]$, **1b**. In the drybox, 2.32 g (0.35 mmol) of **1a** was dissolved in 8 mL of CH_3CN , and 115 mg of NaBF_4 (1.05 mmol, 3.0 equiv) was added to the stirred solution. The initially yellow solution became orange-brown as NaBF_4 dissolved into the solution. After 30 min of stirring, the NaBF_4 had dissolved completely. The solvent was removed in vacuum at room temperature. The resulting dark brown solid was dissolved in 3 mL of CH_3CN and transferred to a 400 mL beaker. To this solution was added 200 mL of ethyl acetate over 10 min in small portions, with vigorous stirring. The product separated first as a gummy material, which gradually turned into an orange-brown powder. The mixture was stirred for 15 min after the final portion of ethyl acetate was added. The orange-brown solid was collected on a frit and washed with 10 mL of ethyl acetate. The filtrate was yellow and slightly cloudy. This precipitation procedure was repeated once. The product was washed with 15 mL of diethyl ether and dried overnight at room temperature in vacuum. Yield: 1.39 g (0.25 mmol, 70%). ¹⁹F NMR (32 scans) showed the presence of ca. 0.28 equiv of contaminating $(n\text{-C}_4\text{H}_9)_4\text{NBF}_4$, δ (no. of F, $\Delta\nu_{1/2}$): -151.1 (1.1 F [= 0.28 equiv of BF_4^-], 1.9 ± 0.1 Hz, singlet).

To remove the remaining 0.28 equiv of $(n\text{-C}_4\text{H}_9)_4\text{NBF}_4$, four additional reprecipitations (six total reprecipitation cycles) from 3 mL of CH_3CN and 200 mL of EtOAc for each cycle were done; after two reprecipitations (four cycles total), the yield was 59%, and 0.05 equiv of $(n\text{-C}_4\text{H}_9)_4\text{NBF}_4$ was detected; after two more reprecipitations (six cycles total), the yield was 53%, and less than 0.01 equiv ($< 1\%$) of $(n\text{-C}_4\text{H}_9)_4\text{NBF}_4$ was detected by ¹⁹F NMR after 256 scans. IR (KBr pellet, cm^{-1}): ν_{CO} 2011 (s), 2000 (sh), 1872 (s), 1888 (sh); polyoxometalate region 1124 (w), 1083 (vs), 1061 (sh), 1013 (w), 948 (s), 939 (s), 915 (sh), 907 (s), 898 (s), 780 (vs). IR (in CH_3CN): see text. ³¹P NMR (33 mM of **1b** plus 99 mM [3.0 equiv] of Kryptofix[2.2.2] in CD_3CN , after heating to 60 °C for 40 min), δ (no. of P, $\Delta\nu_{1/2}$): -7.66 (1P, 1.9 ± 0.1 Hz), -13.30 (1P, 2.3 ± 0.2 Hz). ¹⁹F NMR (256 scans) δ (no. of F, $\Delta\nu_{1/2}$): -151.1 (0.03 F [0.007 equiv of BF_4^-], 1.9 ± 0.1 Hz). ¹⁸³W NMR (80 mM of **1b** in CD_3CN): δ (no. of W, $\Delta\nu_{1/2}$): -128 (3W, 4 ± 1 Hz), -148 (6W, 6 ± 1 Hz), -183 (6W, 3 ± 1 Hz).

Anal. Calcd (found) for $\text{C}_{83}\text{H}_{180}\text{N}_5\text{Na}_3\text{ReP}_2\text{W}_{15}\text{Nb}_3\text{O}_{65}$: C, 17.7 (16.1); H, 3.2 (2.9); N, 1.2 (1.2); Na, 1.2 (1.56); Re, 3.30 (2.29).

$[(n\text{-C}_4\text{H}_9)_4\text{N}]_8[\text{Ir}(1,5\text{-COD})\cdot\text{P}_2\text{W}_{15}\text{Nb}_3\text{O}_{62}]\cdot(n\text{-C}_4\text{H}_9)_4\text{NBF}_4$. The following procedure is based on our preparation of $[(n\text{-C}_4\text{H}_9)_4\text{N}]_5\text{Na}_3[\text{Ir}(1,5\text{-COD})\cdot\text{P}_2\text{W}_{15}\text{Nb}_3\text{O}_{62}]$,^{16j} in the present preparation, however, the isolated iridium complex $[\text{Ir}(1,5\text{-COD})(\text{CH}_3\text{CN})_2]\text{BF}_4$ ²³ was used instead of generating the same complex in situ from $[\text{Ir}(1,5\text{-COD})\text{Cl}]_2$ and AgBF_4 .^{16j} (Use of the isolated complex helps ensure that one can achieve exactly the desired 1.0 $\text{Ir}(1,5\text{-COD})^+$ to 1.0 $\text{P}_2\text{W}_{15}\text{Nb}_3\text{O}_{62}^{9-}$ stoichiometry; this is especially important in the present preparation because the highly soluble all tetrabutylammonium, $[(n\text{-C}_4\text{H}_9)_4\text{N}]_8^{8+}$, product cannot be purified by precipitation from $\text{CH}_3\text{CN}/\text{EtOAc}$ as is possible in the case of the less soluble $[(n\text{-C}_4\text{H}_9)_4\text{N}]_5\text{Na}_3^{8+}$ compound.^{16j})

In the drybox, $[(n\text{-C}_4\text{H}_9)_4\text{N}]_9\text{P}_2\text{W}_{15}\text{Nb}_3\text{O}_{62}$ (3.0 g, 0.48 mmol) was dissolved in CH_3CN (10 mL). To this clear, colorless solution a solution of $[\text{Ir}(1,5\text{-COD})(\text{CH}_3\text{CN})_2]\text{BF}_4$ (225 mg, 0.48 mmol; in 2 mL of CH_3CN) was added dropwise over 3 min. The solution turned orange. After 2.5 h of stirring, the solution was evacuated to dryness in vacuo at room temperature. The orange-yellow residue was dissolved in 3 mL of CH_3CN , and the resultant orange-brown solution was added dropwise to 200 mL of diethyl ether with vigorous stirring. A pale yellow powder formed immediately. After the suspension was stirred for 30 min, the pale yellow powder was collected on a frit, washed with 10 mL of ether, and dried overnight in vacuum. Yield: 2.87 g (0.43 mmol, 90%). IR (KBr pellet, cm^{-1}): 1083 (vs), 1061 (m), 1032 (w), 1012 (w), 940 (s), 914 (s), 891 (s), 776 (vs). ³¹P NMR (33 mM in CD_3CN), δ (no. of P, $\Delta\nu_{1/2}$): -7.08 (1P, 2.5 ± 0.2 Hz), -13.32 (1P, 2.7 ± 0.3 Hz).

(23) (a) The compound $[\text{Ir}(1,5\text{-COD})(\text{CH}_3\text{CN})_2]\text{BF}_4$ was prepared according to the literature method,^{23b} except that AgBF_4 was used instead of AgPF_6 . The product was obtained in 83% yield and characterized by ¹H-NMR. (b) Day, V. W.; Klemperer, W. G.; Main, D. J. *Inorg. Chem.*, **1990**, *29*, 2345–2355.

^{19}F NMR (32 scans), δ (no. of F, $\Delta\nu_{1/2}$): -151.1 (3.6 F [=0.90 equiv of BF_4^-], 2.0 ± 0.1 Hz). Note that no attempt was made to remove the 1.0 equiv of $(n\text{-C}_4\text{H}_9)_4\text{NBF}_4$ in this product (nor in **2a** below), since this was accomplished by preparing the mixed $[(n\text{-C}_4\text{H}_9)_4\text{N}]_5\text{Na}_3^{8+}$ salt, **2b** (*vide infra*). This $[(n\text{-C}_4\text{H}_9)_4\text{N}]_5^{8+}$ salt is, however, a key complex for the NMR and $\text{Ir}(1,5\text{-COD})^+$ and $\text{Ir}(\text{CO})_2^+$ mobility discovery which follows.

$[(n\text{-C}_4\text{H}_9)_4\text{N}]_8[\text{Ir}(\text{CO})_2\cdot\text{P}_2\text{W}_{15}\text{Nb}_3\text{O}_{62}]\cdot(n\text{-C}_4\text{H}_9)_4\text{NBF}_4$, **2a**. In the drybox, $[(n\text{-C}_4\text{H}_9)_4\text{N}]_8[\text{Ir}(1,5\text{-COD})\cdot\text{P}_2\text{W}_{15}\text{Nb}_3\text{O}_{62}]\cdot(n\text{-C}_4\text{H}_9)_4\text{NBF}_4$ (999 mg, 0.15 mmol) and toluene (0.015 mL, as GC internal standard, see below) were dissolved in 4 mL of dry CH_2Cl_2 and placed in a 25 mL Schlenk tube with a 14/20 taper-joint (female) and a glass-stopcock side-arm (Supporting Information, Figure A-a). The Schlenk tube was then connected to an adapter with a taper-joint (male), an O-ring joint (Ace #7) and a Teflon needle valve (Kontes HIVAC). At the same time, 30 mL of dry diethyl ether was placed in another Schlenk tube with a 19/22 taper-joint (male) and a glass-stopcock side-arm (Supporting Information, Figure A-b). This tube was then connected to a fritted filter funnel with two 19/22 taper-joints (both female) and a glass stopcock. On the other end of this filter funnel, another (empty) Schlenk tube, with a 19/22 taper-joint (male) and a glass-stopcock side-arm, was attached as a receiver for the filtrate. The stopcocks were all closed, and then both Schlenk assemblies were taken out of the drybox. (*Caution*: each of the steps with carbon monoxide which follow should be done in a hood!) The Schlenk tube containing the solution of polyoxoanion was connected to the gas-uptake line via the O-ring joint. (The total volume of the gas-uptake line, including the Schlenk tube, had been calibrated beforehand using a calibration flask; detailed procedures are available as Supporting Information). The solution was degassed by three cycles of freeze-pump-thaw, and then placed in a dry ice/ethanol bath. After 15 min, carbon monoxide was introduced (486 Torr) without stirring the solution. The system was then kept standing for 30 min, to make sure that the pressure of carbon monoxide did not change (within ± 1 Torr). The desired reaction with CO was then initiated by stirring the solution vigorously. After 20 min, the CO pressure decreased to 440 Torr, which then remained unchanged (± 1 Torr) for 1 h. The pressure change corresponds to uptake of 0.31 mmol (2.1 ± 0.2 equiv) of CO.

The reaction solution was then slowly transferred (over 3 min) via a stainless-steel cannula under slight pressure of argon into the other Schlenk tube containing ether, which had been cooled to -78°C under argon flow and which was vigorously stirred. A pale yellow solid appeared immediately. The suspension was stirred for 5 min after transfer was completed. The solid was then collected on the frit by turning the whole apparatus upside down and applying a slight pressure of argon on the top side of the frit. When no more liquid was seen coming from the frit, the stopcock between the frit and the filtrate receiver was closed, and the filtrate receiver was detached from the assembly. GC analysis of the colorless, slightly cloudy filtrate revealed 1.1 ± 0.1 equiv of 1,5-cyclooctadiene had been released (see the Instrumentation/Analytical Procedures for details of the GC setup and conditions).

The pale yellow solid was taken into the drybox, where it was transferred to a glass vial and dried overnight at room temperature in vacuum. Yield: 743 mg (0.11 mmol, 75%). IR (KBr pellet, cm^{-1}): ν_{CO} 2046 (s), 1966 (s); polyoxometalate region 1084 (vs), 1062 (m), 940 (s), 911 (s), 895 (s), 809 (sh), 775 (vs), 524 (m). ^{31}P NMR, 33 mM in CD_2Cl_2 , 200 scans, δ (no. of P, $\Delta\nu_{1/2}$): -8.11 (1P, 1.9 ± 0.1 Hz), -13.81 (1P, 2.1 ± 0.1 Hz). ^{31}P NMR, 33 mM in CD_3CN , 200 scans: -7.55 (1P, 1.8 ± 0.1 Hz), -13.12 (1P, 1.9 ± 0.1 Hz). ^{19}F NMR (32 scans), δ (no. of F, $\Delta\nu_{1/2}$): -151.1 (3.8 F [=0.94 equiv of BF_4^-], 4.7 ± 0.1 Hz).

Because of the high sensitivity of **2a** to water (see below), care should be taken to avoid any exposure of **2a** to atmospheric moisture throughout the Schlenk tube or other manipulations outside the drybox.

Stability of 2a. Compound **2a** is moderately stable in solution. Specifically, a 33 mM solution of **2a** in CD_3CN , kept in the drybox at room temperature for 48 h, with or without protection from diffuse room light, showed only a slight change in color (yellow to brown) and in its ^{31}P NMR (small peaks appeared around -7 ppm and -13 ppm). Heating the solution to 60°C for 50 min did not cause any noticeable, further change. On the other hand, addition of 1 equiv of

H_2O to a freshly prepared solution of **2a** caused appearance of new peaks at -5.3 , -6.9 , and -13.3 ppm within 10 min (Supporting Information, Figure H). Although these peaks did not grow further in 1 h at room temperature, they did grow on adding 1 equiv more of H_2O , and grew further after heating at 60°C for 50 min. After the heat treatment, the initially yellow solution turned dark blue (suggestive of the presence of reduced, W^{v} containing, well-known "heteropolyblues"^{21a}). Exposure of another fresh solution of **2a** in CD_3CN to air also caused the appearance of new peaks at -5.3 , -6.9 , and -13.3 ppm (Supporting Information, Figure I).

$[(n\text{-C}_4\text{H}_9)_4\text{N}]_5\text{Na}_3[\text{Ir}(\text{CO})_2\cdot\text{P}_2\text{W}_{15}\text{Nb}_3\text{O}_{62}]$, **2b**. The same procedure as in the preparation of the all tetrabutylammonium salt, **2a**, was followed to prepare this mixed, $[(n\text{-C}_4\text{H}_9)_4\text{N}]_5\text{Na}_3^{8+}$, salt except for the following points: (1) $[(n\text{-C}_4\text{H}_9)_4\text{N}]_5\text{Na}_3[\text{Ir}(1,5\text{-COD})\cdot\text{P}_2\text{W}_{15}\text{Nb}_3\text{O}_{62}]^{16}$ (536 mg, 0.094 mmol) was used as a starting material; (2) CH_3CN (3 mL) was used as solvent instead of CH_2Cl_2 (due to low solubility of the starting material in the latter solvent); and (3) reaction was carried out at 0°C . The amounts of CO consumed (determined manometrically) and 1,5-cyclooctadiene released by GC were 0.18 mmol (1.9 equiv) and 0.099 mmol (1.1 equiv), respectively. The reaction solution was deep red, from which a pink solid was obtained by transferring the solution over 3 min to 30 mL of ether. Yield: 437 mg (0.078 mmol, 83%). IR (KBr pellet, cm^{-1}): ν_{CO} 2047 (s), 1965 (s); polyoxometalate region 1023 (m), 1083 (vs), 1011 (m), 940 (s), 915 (s), 894 (s), 811 (sh), 775 (vs). ^{31}P NMR, 33 mM in CD_3CN : δ -8.42 (3.6 Hz), -8.63 (3.3 Hz), -12.85 (5.3 Hz); a number of smaller signals accompany these dominant signals. ^{31}P NMR, 33 mM with 99 mM (3 equiv) of Kryptofix in CD_3CN , after heating to 60°C for 40 min: δ -7.36 (2.2 Hz), -7.57 (2.2 Hz), -13.13 (2.4 Hz), -13.21 (4.4 Hz); (Figure J, Supporting Information). Anal. Calcd (Found) for $\text{C}_{82}\text{H}_{180}\text{N}_5\text{Na}_3\text{IrP}_2\text{W}_{15}\text{Nb}_3\text{O}_{63}$: C, 17.5 (17.23); H, 3.2 (3.29); N, 1.2 (1.44); Na, 1.2 (1.39); Ir, 3.4 (3.01).

$[(n\text{-C}_4\text{H}_9)_4\text{N}]_8[\text{Rh}(1,5\text{-COD})\cdot\text{P}_2\text{W}_{15}\text{Nb}_3\text{O}_{62}]\cdot(n\text{-C}_4\text{H}_9)_4\text{NBF}_4$. The following procedure is strictly analogous to our published synthesis of the iridium congener, $[(n\text{-C}_4\text{H}_9)_4\text{N}]_5\text{Na}_3[\text{Ir}(1,5\text{-COD})\cdot\text{P}_2\text{W}_{15}\text{Nb}_3\text{O}_{62}]^{16}$. In the drybox, $[\text{Rh}(1,5\text{-COD})\text{Cl}]_2$ (41.4 mg, 0.084 mmol) was dissolved in 3.5 mL of CH_3CN . To this stirred yellow solution was added a solution of fresh AgBF_4 (32.8 mg, 0.168 mmol) in 1 mL of CH_3CN was added by pipette. A white precipitate of AgCl was immediately formed. The mixture was stirred for 30 min. The AgCl precipitated was removed by gravity filtration through Whatman No. 1 paper and the filtrate was introduced directly into the clear, vigorously stirred solution of $[(n\text{-C}_4\text{H}_9)_4\text{N}]_9\text{P}_2\text{W}_{15}\text{Nb}_3\text{O}_{62}$ (1.0 g, 0.16 mmol) in CH_3CN (6.5 mL), which had been previously placed into a 50 mL round-bottomed flask. The filter paper was washed with 1 mL of CH_3CN . The initially colorless polyoxoanion solution turned orange-red at this stage.

Next, the solution was evacuated to dryness in vacuum at room temperature. The orange-yellow residue was dissolved in 1.5 mL of CH_2Cl_2 , and added dropwise over 5 min to vigorously stirred diethyl ether (50 mL). The pale orange precipitate was collected on a medium frit and then washed with diethyl ether. This precipitation procedure was repeated once again, and the orange product was dried overnight in vacuum at room temperature. Yield: 691 mg (0.105 mmol, 66%). ^{31}P NMR (33 mM in CD_3CN), δ (no. of P, $\Delta\nu_{1/2}$): -7.35 (1P, 3.8 ± 0.1 Hz), -13.38 (1P, 3.0 ± 0.1 Hz).

$[(n\text{-C}_4\text{H}_9)_4\text{N}]_8[\text{Rh}(\text{CO})_2\cdot\text{P}_2\text{W}_{15}\text{Nb}_3\text{O}_{62}]\cdot(n\text{-C}_4\text{H}_9)_4\text{NBF}_4$, **3**. The same procedure as in the preparation of the iridium analog, **2a**, was followed to prepare this compound except that $[(n\text{-C}_4\text{H}_9)_4\text{N}]_8[\text{Rh}(1,5\text{-COD})\cdot\text{P}_2\text{W}_{15}\text{Nb}_3\text{O}_{62}]\cdot(n\text{-C}_4\text{H}_9)_4\text{NBF}_4$ (493 mg, 0.075 mmol) was used as starting material and the amount of toluene (GC internal standard) was reduced to 7.5 μL . The amounts of CO consumed and 1,5-cyclooctadiene released were 0.15 mmol (2.0 equiv) and 0.075 mmol (1.0 equiv), respectively. The initially yellow-brown solution turned bright yellow at the end of the reaction. A pale yellow solid was obtained by transferring the solution dropwise over 3 min into 30 mL of ether, which had been cooled to -78°C under argon. It was taken into the drybox, transferred to a glass vial, and dried overnight at room temperature in vacuo. Yield: 314 mg (0.048 mmol, 64%). IR (KBr pellet, cm^{-1}): ν_{CO} 2059 (m), 1984 (m); polyoxometalate region 1125 (m), 1084 (vs), 1063 (m), 938 (s), 913 (sh), 907 (s), 894 (s), 814 (sh), 779 (vs). ^{31}P NMR (33 mM in CD_2Cl_2 , at -60°C), δ (no. of P, $\Delta\nu_{1/2}$):

−8.54 (1P, 3.0 ± 0.1 Hz), −14.17 (1P, 3.2 ± 0.1 Hz). ³¹P NMR (33 mM in CD₃CN, at −40 °C, δ (no. of P, Δν_{1/2}): −8.01 (1P, 3.9 ± 0.1 Hz), −13.59 (1P, 3.0 ± 0.1 Hz).

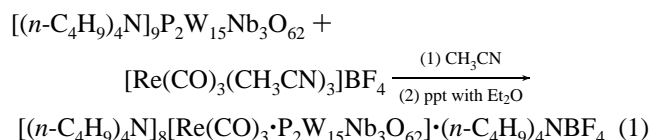
Hydrogenation of Cyclohexene by Photolyzed [(*n*-C₄H₉)₄N]₈[Rh(CO)₂·P₂W₁₅Nb₃O₆₂]·(*n*-C₄H₉)₄NBF₄, **3.** The gas-uptake apparatus shown in Figure B of the Supporting Information was used, except that a larger calibration flask (113 cm³) was used and the stopcock between the calibration flask and the uptake line was left open, so that a larger amount of hydrogen gas can be used (total volume = 224 ± 1 cm³). In the drybox, **3** (50 mg, 7.7 μmol) was dissolved in anhydrous ethanol (2.5 mL, dried over 3 Å molecular sieves), to give a clear, orange-yellow solution. This solution was placed in a side-armed Schlenk tube (Figure A-a, Supporting Information), and cyclohexene (0.5 mL) was added. The solution remained clear and orange-yellow. The stopcocks were closed and the Schlenk tube was taken out of the drybox. The Schlenk tube was attached to the gas-uptake line, and the uptake line was filled with 640 Torr of hydrogen (640 Torr is atmospheric pressure in our mile-high altitude laboratory). Note that the Schlenk tube was still under nitrogen atmosphere at this stage, that is, the reaction solution was not yet degassed. Next, a mineral-oil bubbler was connected to the Schlenk tube via its side arm, and a slow flow (ca. 1 cm³/s) of hydrogen was introduced from the uptake line to the Schlenk tube and exited through the bubbler.

The solution was vigorously stirred and irradiated with a sun lamp (300 W) for 15 min, while maintaining a slow flow of hydrogen. The solution turned dark brown and somewhat cloudy. Irradiation was then turned off, and the hydrogen flow was stopped. The stopcocks to the hydrogen tank and the oil bubbler were closed (*i.e.*, the reaction system was closed with 640 Torr of hydrogen in it).

Stirring of the solution was continued for 12 h, after which time the pressure of hydrogen dropped to 430 Torr. This pressure change corresponds to consumption of ca. 2.5 mmol of hydrogen, although this is only approximate because no attempt was made to keep the temperature constant throughout this initial survey reaction. In the reaction mixture, a fine, black precipitate formed. A sample was collected by allowing the reaction mixture to stand overnight, followed by removal of the slightly cloudy, pale brown supernatant solution by pipet. The remaining black powder in a small amount of solution (ca. 0.5 mL) was centrifuged and the yellow supernatant was removed by pipet. The black powder was then dried under vacuum overnight. The sample (which was soluble in acetone) was shipped to the University of Oregon for TEM analysis, all as detailed previously.^{16f} The results are shown in Figure 12. A GC analysis of the supernatant solution revealed that cyclohexene was completely hydrogenated to cyclohexane (the hydrogen uptake did not match exactly the amount of hydrogen consumed in this initial survey experiment, since part of the starting solution evaporated under a flow of hydrogen gas during the photolysis). Note also that the absolute necessity of photolysis vs mild thermolysis in the generation of the resultant polyoxoanion-stabilized Rh⁰_{*n*} nanoclusters is not revealed by this initial experiment, the intent of which was to confirm our earlier, unpublished observations,^{13f} but with the present, better sample of [Rh(CO)₂·P₂W₁₅Nb₃O₆₂]⁸⁻. More detailed and quantitative experiments generating Rh⁰_{*n*} nanoclusters by this and other reactions are in progress.^{13f}

Results and Discussion

Synthesis, Isolation, and Characterization of [(*n*-C₄H₉)₄N]₈[Re(CO)₃·P₂W₁₅Nb₃O₆₂]·(*n*-C₄H₉)₄NBF₄, **1a.** The target complex [Re(CO)₃·P₂W₁₅Nb₃O₆₂]⁸⁻ was obtained initially as its octakis(tetrabutylammonium) salt by the reaction of [(*n*-C₄H₉)₄N]₉P₂W₁₅Nb₃O₆₂ with [Re(CO)₃(CH₃CN)₃]BF₄ (eq 1).



The product, **1a**, was obtained as a yellow-brown powder. Elemental analysis and ¹⁹F NMR showed that **1a** had not been

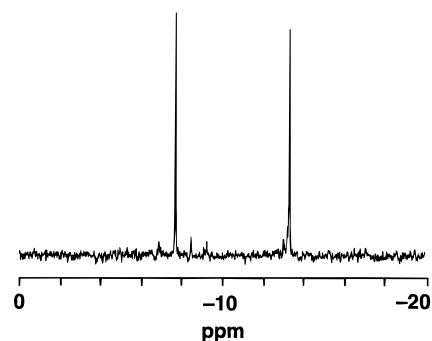


Figure 3. ³¹P NMR spectrum of [(*n*-C₄H₉)₄N]₈[Re(CO)₃·P₂W₁₅Nb₃O₆₂]·(*n*-C₄H₉)₄NBF₄, **1a**, in CD₃CN showing that it is ca. 95% of a single isomer.

separated from the 1 equiv of (*n*-C₄H₉)₄NBF₄ byproduct, eq 1, but, instead, that the isolated solid was a 1:1 mixture of [(*n*-C₄H₉)₄N]₈[Re(CO)₃·P₂W₁₅Nb₃O₆₂] and (*n*-C₄H₉)₄NBF₄. Not unexpectedly, precipitation from a CH₃CN solution by adding ethyl acetate, which had been successfully used in our previous syntheses^{16d,22} of salts containing 7 or less (*n*-C₄H₉)₄N⁺, did not work in this case because of the high solubility of the [(*n*-C₄H₉)₄N]₈⁸⁺ salt of **1a** in this solvent mixture (*i.e.*, no solid material was recovered after adding ethyl acetate; see the Experimental Section for details). Recrystallization from CH₂-Cl₂/EtOAc mixture was also attempted and, indeed, yellow microcrystals were obtained in 22% yield. However, these microcrystals were shown to contain 0.83 equiv of (*n*-C₄H₉)₄NBF₄, that is, only 17% of the contaminating (*n*-C₄H₉)₄NBF₄ had been removed by this procedure. The removal of (*n*-C₄H₉)₄NBF₄ from **1a** by precipitation (or recrystallization) is, therefore, impractical. Nevertheless (*i.e.*, despite the presence of 1 equivalent of (*n*-C₄H₉)₄NBF₄ in the isolated product), complex **1a** is useful and has been included herein for the following reasons: (i) it establishes that a single isomer of supported [Re(CO)₃·P₂W₁₅Nb₃O₆₂]⁸⁻ has been formed (*vide infra*), (2) it indicates that further isolation work, with different cation mixtures to obtain (*n*-C₄H₉)₄NBF₄-free product, was warranted and likely to be successful, and (3) it is quite possible that in some applications (*i.e.*, as EXAFS or other spectroscopic models) this high-solubility, [(*n*-C₄H₉)₄N]₈⁸⁺ salt, **1a**, will be preferred.

A ³¹P NMR spectrum of **1a** in CD₃CN (Figure 3) shows two lines at δ −7.7 and −13.3 with integrated intensities of 1:1; integration of this spectrum also shows that **1a** is at least 95% of a single isomer. The changes in the ³¹P chemical shifts in **1a** from the starting material [(*n*-C₄H₉)₄N]₉P₂W₁₅Nb₃O₆₂ (−6.7 and −13.7 ppm) show the expected downfield shift of the ³¹P (−6.7 ppm) resonance closest to the “Nb₃O₉³⁻” cap in P₂W₁₅Nb₃O₆₂⁹⁻, and provide direct spectroscopic evidence for preferential binding, as expected, of Re(CO)₃⁺ to the more basic “Nb₃O₉³⁻” cap. The observed line widths, Δν_{1/2} = 1.8–2.0 (±0.1) Hz are comparable to those observed for the unsupported polyoxoanion, P₂W₁₅Nb₃O₆₂⁹⁻, which exhibits values for Δν_{1/2} of 1–2 Hz.

Infrared measurements (Figure 4) confirm that the Dawson-type heteropolytungstate framework remains intact under the conditions of the synthesis. The presence of two carbonyl bands (2006 and 1876 cm^{−1}) is consistent with the expected C_{3v} symmetry for the polyoxoanion–Re(CO)₃⁺ complex. These bands have lower frequencies than other Re(CO)₃⁺ complexes with tridentate oxygen ligands, namely [Re(CO)₃·Nb₂W₄O₁₉]³⁻,^{14b} [Re(CO)₃·P₃O₉]²⁻,^{14c} or [CpCo{OP(OEt)₂]₃·Re(CO)₃]²⁺.^{24a} This fact implies that the *quite basic* P₂W₁₅Nb₃O₆₂⁹⁻ ligand is a *stronger donor than other oxo ligands listed above*.

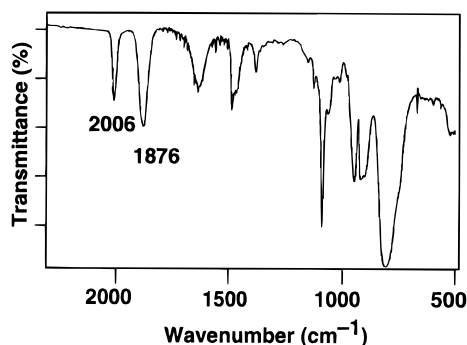


Figure 4. IR spectrum of $[(n\text{-C}_4\text{H}_9)_4\text{N}]_8[\text{Re}(\text{CO})_3\cdot\text{P}_2\text{W}_{15}\text{Nb}_3\text{O}_{62}]\cdot(n\text{-C}_4\text{H}_9)_4\text{NBF}_4$, **1a**, (KBr disk, cm^{-1}) showing the resonances which are characteristic of a Dawson-type heteropolytungstate framework [1083 (vs), 1060 (m), 1010 (w), 941 (s), 913 (s), 896 (s), 798 (vs)] and, in addition, two carbonyl bands at 2006 and 1876 cm^{-1} .

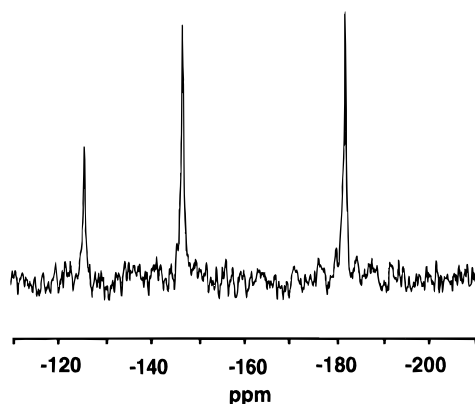


Figure 5. ^{183}W NMR spectrum of $[(n\text{-C}_4\text{H}_9)_4\text{N}]_8[\text{Re}(\text{CO})_3\cdot\text{P}_2\text{W}_{15}\text{Nb}_3\text{O}_{62}]\cdot(n\text{-C}_4\text{H}_9)_4\text{NBF}_4$, **1a**, in CD_3CN . The observed three-line spectrum with relative intensities of 1:2:2 provides direct evidence for the presence of a single isomer, as expected for a complex comprised of an organometallic moiety containing a C_3 axis, such as $[\text{Re}(\text{CO})_3]^+$, and the $\text{P}_2\text{W}_{15}\text{Nb}_3\text{O}_{62}^{9-}$ support-polyoxoanion with its inherent C_{3v} symmetry.

The ^{183}W NMR of **1a** in CD_3CN (Figure 5) shows three peaks, which is also consistent with the preservation of the Dawson-type heteropolytungstate framework and the expected C_{3v} symmetry of the overall molecule, at least on the ^{183}W NMR timescale. The integrated intensities confirm the presence of two tungsten belts consisting of six WO_6 octahedra each and a tungsten cap of three octahedra.

Overall, the above ^{183}W and especially ^{31}P NMR data provide direct evidence that **1a** is a single isomer. As such, complex **1a** is significant: it is discrete, single isomer analog of the well-studied, solid-oxide-supported $\text{Re}(\text{CO})_3^+$. In addition, its tetrabutylammonium counterion composition means that ion-pairing effects, which are well-established to alter spectroscopic properties,^{16d} *vide infra*, are minimized. Because **1a** is a single isomer, efforts to remove the 1 equiv of $(n\text{-C}_4\text{H}_9)_4\text{NBF}_4$ present were undertaken next.

Synthesis, Isolation, and Characterization of the Mixed Cation Salt $[(n\text{-C}_4\text{H}_9)_4\text{N}]_5\text{Na}_3[\text{Re}(\text{CO})_3\cdot\text{P}_2\text{W}_{15}\text{Nb}_3\text{O}_{62}]$, **1b.** Previously, we developed a “mixed-cation” technique using $(n\text{-C}_4\text{H}_9)_4\text{N}^+/\text{Na}^+$, along with precipitation in $\text{EtOAc}/\text{CH}_3\text{CN}$, to remove any $(n\text{-C}_4\text{H}_9)_4\text{NBF}_4$ contaminant^{16d,22} (this works since the $(n\text{-C}_4\text{H}_9)_4\text{NBF}_4$ is very soluble in EtOAc , and the addition of Na^+ to the polyoxoanion lowers its solubility in $\text{EtOAc}/\text{CH}_3\text{CN}$).

In the case of **1a**, the addition of 3 equiv of NaBF_4 to a solution of **1a** in CH_3CN , followed by removal of solvent and two precipitation cycles from $\text{CH}_3\text{CN}/\text{EtOAc}$, a pale brown solid

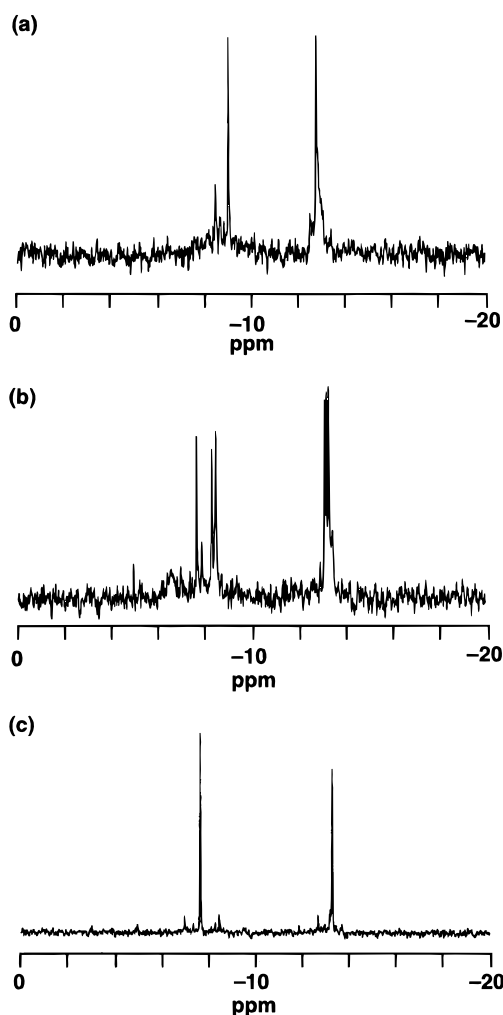


Figure 6. ^{31}P NMR spectra of $[(n\text{-C}_4\text{H}_9)_4\text{N}]_5\text{Na}_3[\text{Re}(\text{CO})_3\cdot\text{P}_2\text{W}_{15}\text{Nb}_3\text{O}_{62}]$, **1b**, in CD_3CN : (a) in the absence of Kryptofix[2.2.2]; (b) after addition of 3 equiv of Kryptofix[2.2.2] at room temperature; (c) after the heating of solution b to 60 °C for 40 min.

of **1b** was obtained in 80% yield. To quantitate the amount of any remaining $(n\text{-C}_4\text{H}_9)_4\text{NBF}_4$, we developed a simple but effective ^{19}F NMR method involving quantitation of the remaining BF_4^- ($\delta = -151.1$ in CD_3CN) vs a PF_6^- internal standard ($\delta = -72.3$ in CD_3CN). This method is more sensitive than the IR method we developed and used previously^{16d,i,j} and, hence, is what we use hereafter and also recommend to others (see the Experimental Section for further details). ^{19}F NMR showed that the mixed cation, $\text{EtOAc}/\text{CH}_3\text{CN}$ precipitation procedure did, as expected, remove much (70–85%) of the $(n\text{-C}_4\text{H}_9)_4\text{NBF}_4$, although ca. 15–30% of the BF_4^- still remained, even after 2 precipitations (Figure F, Supporting Information). This in turn means that complete purification is possible, but is just a trade-off in yield vs purity. As proof of this principle, four further precipitations from $\text{EtOAc}/\text{CH}_3\text{CN}$ (six precipitations total) provided an overall yield of 53% of product, **2**, that was $\geq 99\%$ BF_4^- free by the sensitive ^{19}F NMR method.

The ^{31}P NMR spectra of **1b** were obtained, as usual,^{16d,22} in the presence and absence of 3 equiv of Kryptofix[2.2.2] in CD_3CN (Figure 6), where the cryptand removes ion-pairing effects which otherwise complicate ^{31}P NMR spectra as previously demonstrated.^{16d} The spectrum in the absence of Kryptofix[2.2.2] was broad and multiline (Figure 6a), as expected and as previously observed in $[(n\text{-C}_4\text{H}_9)_4\text{N}]_5\text{Na}_3[(1,5\text{-COD})\text{M}\cdot\text{P}_2\text{W}_{15}\text{Nb}_3\text{O}_{62}]$ (M = Ir and Rh) due to $\text{Na}^+\cdots\text{P}_2\text{W}_{15}\text{Nb}_3\text{O}_{62}^{9-}$ ion-pairing effects.^{16j} After addition of 3 equiv of Kryptofix[2.2.2] at room temperature, the spectrum became sharper, but, interest-

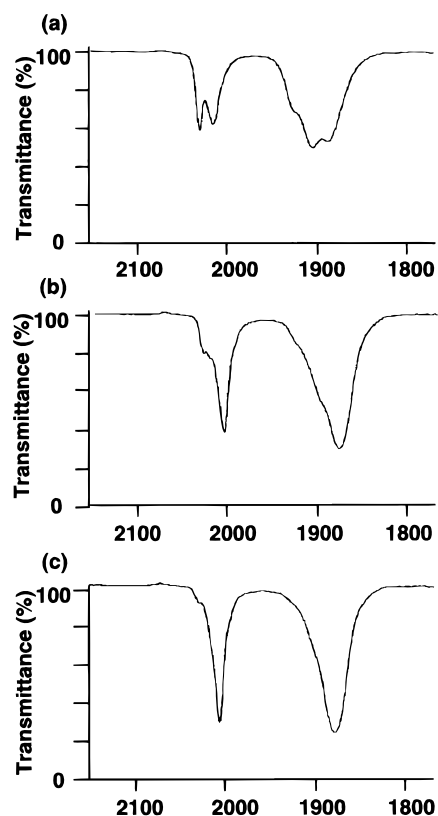


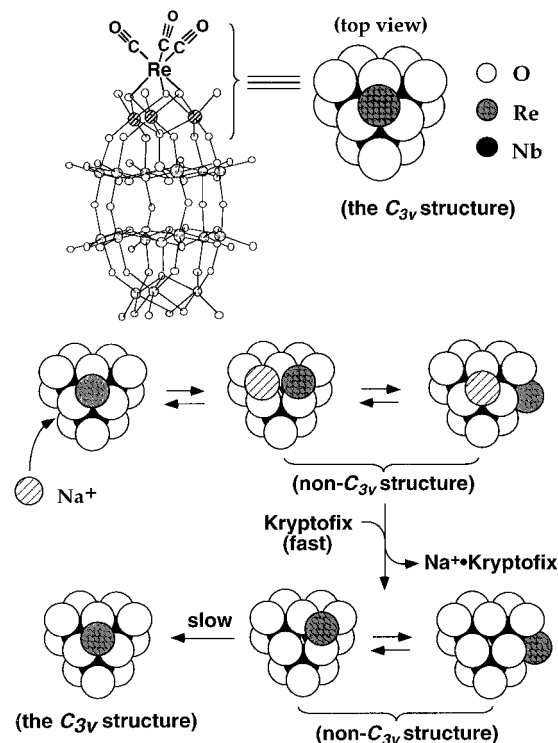
Figure 7. IR spectra of $[(n\text{-C}_4\text{H}_9)_4\text{N}]_5\text{Na}_3[\text{Re}(\text{CO})_3\cdot\text{P}_2\text{W}_{15}\text{Nb}_3\text{O}_{62}]$, **1b**, in CH_3CN (NaCl cell): (a) in the absence of Kryptofix[2.2.2]; (b) after addition of 3 equiv of Kryptofix[2.2.2] at room temperature; (c) after the heating of solution b to $60\text{ }^\circ\text{C}$ for 40 min.

ingly, still showed at least three resonances for each of the two phosphorus atoms (Figure 6b). We anticipated that heating might allow conversion to a single isomer, and indeed, *heating this solution to $60\text{ }^\circ\text{C}$ for 40 min* yielded a clean, two-line spectrum, Figure 6c. Moreover, the chemical shifts of the two signals were identical with those of the all tetrabutylammonium salt, **1a**, within experimental error (-7.7 and -13.4 ppm), as one would expect. Prolonged heating (at $60\text{--}70\text{ }^\circ\text{C}$, up to 7 h) did not further change the ^{31}P NMR spectrum. The ^{183}W NMR, after being heated at $70\text{ }^\circ\text{C}$ for 5 h, showed a three-line ^{183}W NMR, as expected for C_{3v} symmetry (and, again, with identical chemical shifts vs those of **1a** within a ± 2 ppm experimental error).

The IR spectra in CH_3CN solution showed changes analogous to those of the ^{31}P NMR spectra (Figure 7). The CH_3CN solution of **1b**, without Kryptofix, showed two sets of split bands (2028 and 2012 cm^{-1} ; 1920 , 1904 , and 1886 cm^{-1}) in the carbonyl region (Figure 7a), which shifted to higher wavenumbers than the carbonyl bands of **1a** (2006 and 1876 cm^{-1}). After the addition of 3 equiv of Kryptofix[2.2.2] at room temperature, these bands became smaller and two new bands appeared at 2006 and 1876 cm^{-1} (Figure 7b). Finally, after the solution was heated at $60\text{ }^\circ\text{C}$ for 40 min, the spectrum looked exactly the same as that of **1a** (Figure 7c), the expected IR spectrum for a C_{3v} symmetry $\text{Re}(\text{CO})_3^+$ moiety.

As already noted, the additional peaks in the IR and NMR spectra of **1b**, in the absence of added Kryptofix[2.2.2], are due to the effects^{16d} of Na^+ ion-pairing with the polyanionic $[\text{Re}(\text{CO})_3\cdot\text{P}_2\text{W}_{15}\text{Nb}_3\text{O}_{62}]^{8-}$. However, the *slow spectral changes* observed following the addition of Kryptofix[2.2.2] are *without precedent*, and stand in considerable contrast to the faster changes in the case of $[\text{M}(\text{1,5-COD})\cdot\text{P}_2\text{W}_{15}\text{Nb}_3\text{O}_{62}]^{8-}$ (where the spectral changes are complete within *30 min at room*

Scheme 1. C_{3v} Symmetry Structure of $[\text{Re}(\text{CO})_3\cdot\text{P}_2\text{W}_{15}\text{Nb}_3\text{O}_{62}]^{8-}$, **1**, and Its Na^+ Cation-Induced Symmetry Change to Non- C_{3v} Symmetry^a



^a The exact structures of the non- C_{3v} isomer(s) are *not* known and thus are only given as a guide to the needed additional studies.

temperature). One conceivable, but unlikely, explanation for these unusual observations is a slow reaction between Na^+ and Kryptofix[2.2.2] (i.e., a slow removal of predated^{16d} ion-pairing effects between Na^+ and $[\text{Re}(\text{CO})_3\cdot\text{P}_2\text{W}_{15}\text{Nb}_3\text{O}_{62}]^{8-}$). However, this explanation was ruled out by an examination of the ^1H NMR after the addition of Kryptofix. This NMR experiment clearly shows, as expected, that the Kryptofix reacts *immediately* with Na^+ after its addition (i.e., no peaks due to free Kryptofix, easily distinguishable in a control experiment, are observed; see Figure D, Supporting Information). Hence, given the slower timescale of the spectral changes, the only other explanation consistent with all the data, at least that we can see, is that, in the presence of Na^+ , the $[(\text{Re}(\text{CO})_3^+)(\text{Na}^+)\text{P}_2\text{W}_{15}\text{Nb}_3\text{O}_{62}^{9-}]^{7-}$ complex *has non- C_{3v} symmetry*.²⁵ The addition of Kryptofix then binds Na^+ immediately (as proved above), but the change to the C_{3v} symmetry structure established for the *Na^+ -free*, all tetrabutyl ammonium salt, $[\text{Re}(\text{CO})_3\cdot\text{P}_2\text{W}_{15}\text{Nb}_3\text{O}_{62}]^{8-}$ (i.e., established for **1a**) is *slow*. This explanation also makes sense intuitively: the monocations $\text{Re}(\text{CO})_3^+$ and Na^+ are in competition for the most basic, “ $\text{Nb}_3\text{O}_3^{3-}$ ”, binding and support site in $\text{P}_2\text{W}_{15}\text{Nb}_3\text{O}_{62}^{9-}$. This necessarily results in a non- C_{3v} symmetry complex, since both monocations cannot simultaneously bind at the single C_{3v} site atop $\text{P}_2\text{W}_{15}\text{Nb}_3\text{O}_{62}^{9-}$.

The C_{3v} to non- C_{3v} symmetry changes induced by the Na^+ cation are summarized in Scheme 1, along with two plausible and partially predated^{16m} but unproved structures for the non-

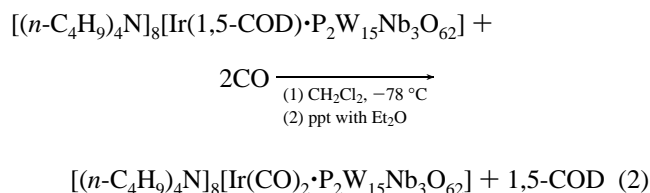
(24) (a) Kläui, W.; Okuda, J.; Scotti, M.; Valderrama, M. *J. Organometallic Chem.* **1985**, *280*, C26. (b) Kläui, W.; Scotti, M.; Valderrama, M.; Rojas, S.; Sheldrick, G. M.; Jones, P. G.; Schroeder, T. *Angew. Chem., Int. Ed. Engl.* **1985**, *24*, 683.

(25) It is possible that ^{17}O NMR or, ideally, a single-crystal X-ray diffraction structural analysis of $[(\text{Re}(\text{CO})_3^+)(\text{Na}^+)\text{P}_2\text{W}_{15}\text{Nb}_3\text{O}_{62}^{9-}]^{7-}$ will provide direct structural insight for or against this proposal. Hence, such additional studies are an important goal of future work.

C_{3v} isomers of $[\text{Re}(\text{CO})_3 \cdot \text{P}_2\text{W}_{15}\text{Nb}_3\text{O}_{62}]^{8-}$. We emphasize that only the non- C_{3v} symmetry of these isomers is known with certainty; hence, Scheme 1 is speculative with respect to the exact structures of these non- C_{3v} symmetry isomers. Scheme 1 is thus offered as a visual summary of both what is and what is not known and, therefore, of the needed additional studies.

These results are not trivial. Instead, they provide the first direct evidence that the overall symmetry of organometallic cations supported on soluble basic oxides can be changed by the presence of cations such as Na^+ (cations that are often "promoters" in heterogeneous catalysis recipes). In addition, a discrete, well-characterized system, $[(n\text{-C}_4\text{H}_9)_4\text{N}]_5\text{Na}_3[\text{Re}(\text{CO})_3 \cdot \text{P}_2\text{W}_{15}\text{Nb}_3\text{O}_{62}]$, **1b** (or, possibly better, the mono- Na^+ salt, $[(\text{Re}(\text{CO})_3^+)(\text{Na}^+)\text{P}_2\text{W}_{15}\text{Nb}_3\text{O}_{62}^{9-}]^{7-}$), is now available for a kinetic, mechanistic and ΔH^\ddagger and ΔS^\ddagger activation parameter studies of $\text{Re}(\text{CO})_3^+$ and other metal cation mobility across a well-characterized, discrete (polyoxoanion) oxide material. Very little is known about how metal cations move across either soluble or solid-oxide surfaces (a fact confirmed by a CAS on-line literature search), although it is clear from the literature that metal cations such as $\text{Rh}(\text{CO})_2^+$ are mobile on solid oxides such as Al_2O_3 .^{2b,4,5,10} We note here the two precedents in polyoxoanion chemistry for organometallic cation mobility on polyoxoanion soluble oxides: Klemperer's work involving an addition/elimination mechanism in the case of $[\text{Cp}^*\text{Rh}^{\text{III}}]^{2+}$ and $\text{Nb}_2\text{W}_4\text{O}_{19}^{4-}$,^{14e} plus a very recent, important report from Yagasaki and co-workers suggesting that $(\eta_4\text{-C}_6\text{H}_{10})\text{Rh}^+$ can pivot when attached to a $\text{V}_4\text{O}_{12}^{4-}$ soluble oxide fragment in the complex $\{[(\eta_4\text{-C}_6\text{H}_{10})\text{Rh}]_2 \cdot \text{V}_4\text{O}_{12}\}^{2-}$.^{26b} Simple fluxionality of organometallics attached to polyoxoanion fragments is more common, of course, for example Klemperer and Day's^{14f} $[(1,5\text{-COD})\text{Ir} \cdot \text{P}_3\text{O}_9]^{2-}$ or Attanasio and co-worker's^{26a} $[(1,5\text{-COD})(\text{CH}_3\text{-CN})\text{Ru}(\text{II}) \cdot \text{P}_3\text{O}_9]^-$.

Synthesis, Isolation, and Characterization of $[(n\text{-C}_4\text{H}_9)_4\text{N}]_8[\text{Ir}(\text{CO})_2 \cdot \text{P}_2\text{W}_{15}\text{Nb}_3\text{O}_{62}] \cdot (n\text{-C}_4\text{H}_9)_4\text{NBF}_4$, **2a.** The conceptually simplest route to the polyoxoanion-supported iridium carbonyl $[\text{Ir}(\text{CO})_2 \cdot \text{P}_2\text{W}_{15}\text{Nb}_3\text{O}_{62}]^{8-}$ is the reaction of carbon monoxide with the well-known 1,5-cyclooctadiene complex $[\text{Ir}(1,5\text{-COD}) \cdot \text{P}_2\text{W}_{15}\text{Nb}_3\text{O}_{62}]^{8-}$ (eq 2).^{16h,17}



The previously unknown all tetrabutylammonium salt, $[(n\text{-C}_4\text{H}_9)_4\text{N}]_8[\text{Ir}(1,5\text{-COD}) \cdot \text{P}_2\text{W}_{15}\text{Nb}_3\text{O}_{62}]$, was prepared and characterized following our well-established methods to give the mixed $[(n\text{-C}_4\text{H}_9)_4\text{N}]_5\text{Na}_3^{8+}$ salt.^{16h,17} It was then allowed to react with carbon monoxide (486 Torr) in CH_2Cl_2 at -78°C for 1.5 h (the reaction was complete within 20 min). The pale yellow powder of **2a** was obtained in 75% yield by precipitation with diethyl ether. The uptake of 2.0 ± 0.2 equiv of carbon monoxide and the release of 1.0 ± 0.1 equiv of 1,5-cyclooctadiene were confirmed by manometry and GC measurements, respectively.

The ^{31}P NMR (Figure 8) in CD_3CN solution showed a clean, two-line spectrum (-7.6 and -13.2 ppm) at room temperature. The infrared spectrum (KBr pellet, Figure 9) shows two sharp

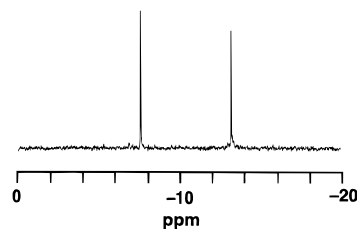


Figure 8. ^{31}P NMR spectrum of $[(n\text{-C}_4\text{H}_9)_4\text{N}]_8[\text{Ir}(\text{CO})_2 \cdot \text{P}_2\text{W}_{15}\text{Nb}_3\text{O}_{62}] \cdot (n\text{-C}_4\text{H}_9)_4\text{NBF}_4$, **2a**, in CD_3CN .

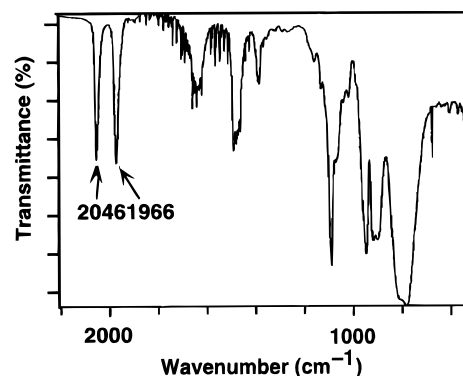


Figure 9. IR spectrum (KBr pellet) of $[(n\text{-C}_4\text{H}_9)_4\text{N}]_8[\text{Ir}(\text{CO})_2 \cdot \text{P}_2\text{W}_{15}\text{Nb}_3\text{O}_{62}] \cdot (n\text{-C}_4\text{H}_9)_4\text{NBF}_4$, **2a**.

carbonyl bands at 2046 and 1966 cm^{-1} characteristic of *gem*-dicarbonyl species of C_s symmetry.

The $[\text{Ir}(\text{CO})_2 \cdot \text{P}_2\text{W}_{15}\text{Nb}_3\text{O}_{62}]^{8-}$ product, **2a**, is moderately stable in CD_3CN . After a solution was allowed to stand for 48 h in room temperature CD_3CN (with or without protection from diffuse room light), we observed a set of new, although small, ^{31}P peaks around -7 ppm (Supporting Information, Figure G). The color of the solution also changed from yellow to brown. Heating this solution to 60°C for 50 min did not cause further substantial change.

A more rapid and definitive change was observed when H_2O or O_2 was deliberately added. Addition of 1 equiv of H_2O or a fresh CD_3CN solution of **2a** caused appearance of a few new ^{31}P peaks within 15 min (Supporting Information, Figure H). Exposure to air of another fresh CD_3CN solution of **2a** also caused appearance of new peaks within 30 min (Supporting Information, Figure I).

Preparation and Isomer Characterization of the Mixed Salt, $[(n\text{-C}_4\text{H}_9)_4\text{N}]_5\text{Na}_3[\text{Ir}(\text{CO})_2 \cdot \text{P}_2\text{W}_{15}\text{Nb}_3\text{O}_{62}]$, **2b.** In an attempt to remove the contaminating 1 equiv of $(n\text{-C}_4\text{H}_9)_4\text{NBF}_4$ in **2a**, we tried to prepare the mixed $[(n\text{-C}_4\text{H}_9)_4\text{N}]_5\text{Na}_3^{8+}$ salt of $[\text{Ir}(\text{CO})_2 \cdot \text{P}_2\text{W}_{15}\text{Nb}_3\text{O}_{62}]^{8-}$. The well-established, fully characterized compound $[(n\text{-C}_4\text{H}_9)_4\text{N}]_5\text{Na}_3[\text{Ir}(1,5\text{-COD}) \cdot \text{P}_2\text{W}_{15}\text{Nb}_3\text{O}_{62}]^{16j}$ was allowed to react with carbon monoxide (486 Torr) in CH_3CN at 0°C . The brown-yellow solution turned deep red within 30 min, and a pink solid was obtained after precipitation by diethyl ether (83% yield). The infrared spectrum (KBr pellet) showed two sharp carbonyl bands at 2047 and 1965 cm^{-1} characteristic of *gem*-dicarbonyl species of C_s symmetry.

The ^{31}P NMR of **2b** in CD_3CN , Figure 10, also showed the same, "slow spectroscopic changes" detailed above after the addition of Kryptofix, but the final spectrum was slightly more complicated than that of the $\text{Re}(\text{CO})_3^+$ compound, **1b** (not unexpectedly; note that $\text{Ir}(\text{CO})_2^+$ is a 2-fold rotor whereas the 3-fold rotor $\text{Re}(\text{CO})_3^+$ matches the polyoxoanion's 3-fold symmetry, " $\text{Nb}_3\text{O}_9^{3-}$ " site). Specifically, the ^{31}P NMR in CD_3CN without added Kryptofix showed two sets of multiple lines around -8 ppm and -13 ppm, Figure 10a. Upon addition of

(26) (a) Attanasio, D.; Bachechi, F.; Suber, L. *J. Chem. Soc., Dalton Trans.* **1993**, 2373. (b) Abe, M.; Isobe, K.; Kida, K.; Yagasaki, A. *Inorg. Chem.* **1996**, 35, 5114.

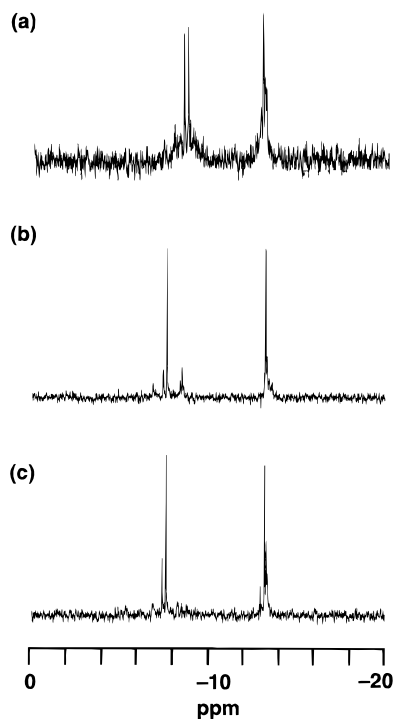


Figure 10. ^{31}P NMR of $[(n\text{-C}_4\text{H}_9)_4\text{N}]_5\text{Na}_3[\text{Ir}(\text{CO})_2\cdot\text{P}_2\text{W}_{15}\text{Nb}_3\text{O}_{62}]$, **2b**, in CD_3CN at room temperature: (a) in the absence of Kryptofix[2.2.2]; (b) after addition of 3 equiv of Kryptofix[2.2.2]; (c) after heating solution b to $60\text{ }^\circ\text{C}$ for 40 min.

3 equiv of Kryptofix, a new signal appeared at -7.6 ppm while the signals at -8 ppm were still observed, Figure 10b. Heating this solution at $60\text{ }^\circ\text{C}$ for 40 min gave a predominantly four-line spectrum, Figure 10c, in which the two major sets of species (i.e., with two ^{31}P lines per polyoxoanion) are present in an estimated 70:30 ratio (based on the ^{31}P NMR integral intensities). The chemical shifts of the major species (-7.6 and -13.2 ppm) were identical within experimental error with those of the all-tetrabutylammonium salt, **2a**.

The presence of Na^+ in **2b** is the obvious explanation for the additional ^{31}P NMR lines in comparison to the clean, two-line spectrum seen for the all- $(n\text{-C}_4\text{H}_9)^+$ salt, **2a** (recall Figure 8). Hence, a control experiment (hereafter, control A) was performed in which 3 equiv of NaBF_4 was added to **2a**. Specifically, the addition of 3 equiv of NaBF_4 to a yellow solution of the all- $(n\text{-C}_4\text{H}_9)^+$ salt **2a** in CD_3CN gave a deep-red solution. After this solution was stirred for 12 h at room temperature and heated at $60\text{ }^\circ\text{C}$ for 40 min, the resultant solution exhibited a ^{31}P NMR spectrum similar to that observed for a CD_3CN solution of **2b**, Figure 11a. The addition of 3 equiv of Kryptofix changed this spectrum some, but failed to convert it into a cleaner spectrum in the absence of heating, Figure 11b. Heating this solution to $60\text{ }^\circ\text{C}$ for 50 min yielded a predominantly clean two-line ^{31}P spectrum, which was observed to have chemical shifts identical to those for **2b** within experimental error, Figure 11c. *However*, the amount of the minor species was 5%, instead of 30% as in the case of **2b** (i.e., compare Figures 11c and 10c). Further heating of this solution ($60\text{ }^\circ\text{C}$, 40 min) did not change the ratio of the two species. This control experiment establishes two points: (a) the presence of Na^+ is responsible for the extra lines seen in the ^{31}P NMR of **2b** in comparison to **2a**; and (b) conversion to the two-line, apparently C_{3v} spectrum seen for the all-tetrabutylammonium salt, **2a**, requires heating—that is, it is *slow*. Another control experiment (control B) using **2a** and 3 equiv of NaBF_4 was done, under the same conditions as described for control A, except that Kryptofix was added after stirring

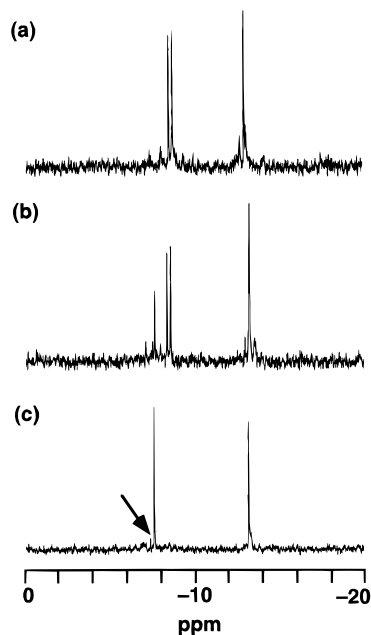


Figure 11. ^{31}P NMR of $[(n\text{-C}_4\text{H}_9)_4\text{N}]_8[\text{Ir}(\text{CO})_2\cdot\text{P}_2\text{W}_{15}\text{Nb}_3\text{O}_{62}]^+(n\text{-C}_4\text{H}_9)_4\text{NBF}_4^-$, **2a**, in CD_3CN at room temperature, with various additives (control A, see text): (a) after the addition of 3 equiv of NaBF_4 and allowing the solution to stand for 12 h at room temperature followed by heating to $60\text{ }^\circ\text{C}$ for 40 min; (b) 30 min after the addition of 3 equiv of Kryptofix[2.2.2] to solution a; (c) after heating solution b for 50 min at $60\text{ }^\circ\text{C}$. The arrow indicates the signal of the minor isomer.

the mixture of **2a** and NaBF_4 for 2 h at room temperature (instead of stirring for 12 h and heating). Our goal here was to test whether or not, as suspected, heating is also required to form the extra isomers seen in **2b**. In this control experiment, the final spectrum was a clean, two-line one, thereby demonstrating the absence of the minor species (Figure J, Supporting Information). The consistent interpretation here (i.e., after also considering the data in Figures 10 and 11) is that the second isomer seen with **2b** is *never formed in this control experiment* due to the deliberate omission of heating the sample.

These results indicate, in turn, that (a) there are two isomers present for $\text{Ir}(\text{CO})_2^+$ supported on $\text{P}_2\text{W}_{15}\text{Nb}_3\text{O}_{62}^{9-}$, (b) that the non- C_{3v} isomer is induced by the addition of a second cation, such as Na^+ , plus heating, and (c) conversion back to the C_{3v} isomer is also *slow* and requires heating after the removal of the Na^+ using Kryptofix. In short, there is a sizable kinetic barrier between interconversion of the two isomers of $\text{P}_2\text{W}_{15}\text{Nb}_3\text{O}_{62}^{9-}$ supported $\text{Ir}(\text{CO})_2^+$.

Two other insights are apparent following reflection upon these results and some of our earlier work. Apparently, $[(n\text{-C}_4\text{H}_9)_4\text{N}]_5\text{Na}_3[\text{Ir}(1,5\text{-COD})\cdot\text{P}_2\text{W}_{15}\text{Nb}_3\text{O}_{62}]$ exists as a mixture of two isomers in CH_3CN solution (i.e., in the absence of Kryptofix and thus in the presence of the effects of Na^+). This follows since the requirement for heating herein for interconversion of supported $\text{Ir}(\text{CO})_2^+$ isomers renders it very unlikely that the minor, 30% species in **2b** has been formed under the mild, 1.5 h at $0\text{ }^\circ\text{C}$, synthetic conditions. This explanation is consistent with our previous results^{16j} showing that $[(n\text{-C}_4\text{H}_9)_4\text{N}]_5\text{Na}_3[\text{Ir}(1,5\text{-COD})\cdot\text{P}_2\text{W}_{15}\text{Nb}_3\text{O}_{62}]$ in CD_3CN without addition of Kryptofix exhibits multiple ^{31}P signals; we had just never before had results that demanded an interpretation over and above the usual ion-pairing effects. Second, both $\text{Ir}(1,5\text{-COD})^+$ as well as $\text{Ir}(\text{CO})_2^+$ are mobile about or on the “ $\text{Nb}_3\text{O}_9^{3-}$ ” cap in $\text{P}_2\text{W}_{15}\text{Nb}_3\text{O}_{62}^{9-}$, but with $\text{Ir}(1,5\text{-COD})^+$ being more mobile than $\text{Ir}(\text{CO})_2^+$. Evidence for this comes from the ^{31}P NMR of $[(n\text{-C}_4\text{H}_9)_4\text{N}]_5\text{Na}_3[\text{Ir}(1,5\text{-COD})\cdot\text{P}_2\text{W}_{15}\text{Nb}_3\text{O}_{62}]$ in CD_3CN after ad-

dition of 3 equiv of Kryptofix. The spectrum collapses quickly (*i.e.* within 30 min at room temperature) to a two-line spectrum indicating a single isomer (*i.e.*, on the ^{31}P NMR time scale).^{16j} These mild conditions contrast with the 35 °C higher (60 °C) temperature required to interconvert the isomers of **2b**. The higher mobility of $\text{Ir}(1,5\text{-COD})^+$ over that for $\text{Ir}(\text{CO})_2^+$ about the “ $\text{Nb}_3\text{O}_9^{3-}$ ” cap is, of course, reasonable given the stronger π -accepting nature of carbonyl ligands and their anticipated synergistic interaction with the electron-donating oxygens atop $\text{P}_2\text{W}_{15}\text{Nb}_3\text{O}_{62}^{9-}$.

Preparation and Isolation of the Unstable Rhodium Dicarboxyl Congener $[(n\text{-C}_4\text{H}_9)_4\text{N}]_8[\text{Rh}(\text{CO})_2\cdot\text{P}_2\text{W}_{15}\text{Nb}_3\text{O}_{62}]$, **3**. We also synthesized and isolated at low temperature the analogous $\text{P}_2\text{W}_{15}\text{Nb}_3\text{O}_{62}^{9-}$ -supported $\text{Rh}(\text{CO})_2^+$ complex, as it is one of the best studied, solid-oxide-supported $\text{M}(\text{CO})_n^+$ from among the three better studied monometallic carbonyls, $\text{Re}(\text{CO})_3^+$, $\text{Ir}(\text{CO})_2^+$, and $\text{Rh}(\text{CO})_2^+$. Indeed, our studies actually began here long ago,^{13f} but our concern about the unstable nature of this complex, a concern validated by the results which follow, caused us to return to this $\text{Rh}(\text{CO})_2^+$ complex only after the data on the more stable $\text{Re}(\text{CO})_3^+$ and $\text{Ir}(\text{CO})_2^+$ analogs were in hand.

The previously unreported all tetrabutylammonium salt, $[(n\text{-C}_4\text{H}_9)_4\text{N}]_8[\text{Rh}(1,5\text{-COD})\cdot\text{P}_2\text{W}_{15}\text{Nb}_3\text{O}_{62}]$, was prepared and characterized following our well-established methods for the $[(n\text{-C}_4\text{H}_9)_4\text{N}]_5\text{Na}_3$ complex.^{16j} In a largely optimized experiment that followed several survey experiments (*i.e.*, mostly at higher temperature and for longer times, following input from what was successful in the support of the $\text{Re}(\text{CO})_3^+$ and closely analogous $\text{Ir}(\text{CO})_2^+$ cation), the well-established precursor^{16j} $[(n\text{-C}_4\text{H}_9)_4\text{N}]_8[\text{Rh}(1,5\text{-COD})\cdot\text{P}_2\text{W}_{15}\text{Nb}_3\text{O}_{62}]$ was allowed to react with carbon monoxide in CH_2Cl_2 at -78 °C for 90 min (the majority of the reaction was complete within 30 min). A pale yellow powder was obtained in 64% yield by the procedure detailed in the Experimental Section. The infrared spectrum (KBr pellet, Figure K, Supporting Information) showed two sharp carbonyl bands at 2059 and 1984 cm^{-1} characteristic of *gem*-dicarbonyl species of C_s symmetry. Product **3** is stable in CD_2Cl_2 at -60 °C for at least 2 h as monitored by ^{31}P NMR, exhibiting two main peaks at -8.5 ppm and -14.2 ppm (Figure L, part a, Supporting Information). At -40 °C the ^{31}P NMR of this material in CD_3CN showed two main peaks at -8.0 and -13.6 ppm (Figure M, part a, Supporting Information). Both spectra show impurity peaks; the relative ^{31}P integrals indicated a purity of ca. 80%, even in these low temperature CD_3CN or CD_2Cl_2 spectra. Note, however, that the reaction with carbon monoxide is complete, since the expected stoichiometry of CO uptake and 1,5-cyclooctadiene release was observed within $\pm 5\%$ (2.0 and 1.0 equiv, respectively). In addition, although the ^{31}P NMR spectrum in CD_3CN (Figure M, Supporting Information) remained unchanged for 2.5 h at -40 °C, *warming to room temperature led to decomposition within 30 min* (broadening of the lower-field ^{31}P signal and change in solution color from yellow to dark brown). A similar change was observed in $\text{CD}_2\text{-Cl}_2$ (Figure L, Supporting Information). It follows, therefore, that the product **3** is unavoidably partially decomposed during the workup. Given the unstable nature of **3** in solution, we can now rationalize our earlier, mostly unsuccessful results from higher temperature and longer time synthetic attempts.^{13f}

The above results too are of more than of just passing interest. They definitively show, for the first time, the low stability of $\text{Rh}(\text{CO})_2^+$ (on at least the very basic $\text{P}_2\text{W}_{15}\text{Nb}_3\text{O}_{62}^{9-}$ oxide and in solution), and also clearly demonstrate the difference between $\text{Rh}(\text{CO})_2^+$ and the more stable $\text{Ir}(\text{CO})_2^+$ and $\text{Re}(\text{CO})_3^+$. In

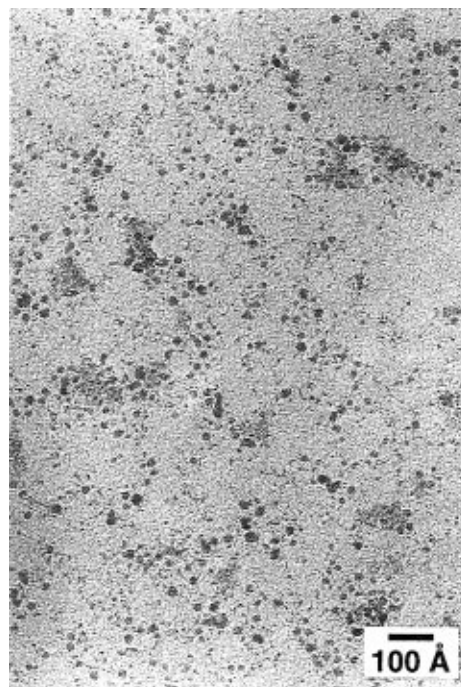


Figure 12. TEM (transmission electron micrograph) of the ca. 10–40 Å Rh_n^0 nanoclusters formed by photolysis of $[(n\text{-C}_4\text{H}_9)_4\text{N}]_8[\text{Rh}(\text{CO})_2\cdot\text{P}_2\text{W}_{15}\text{Nb}_3\text{O}_{62}]\cdot(n\text{-C}_4\text{H}_9)_4\text{NBF}_4$, **3**, under H_2 in anhydrous EtOH and in the presence of cyclohexene. The sample was deposited on a carbon-coated Cu grid, and the TEM obtained on a Philips CM-12 instrument with a 70- μm lens operating at 100 kV by Dr. Eric Schabtach at the University of Oregon Electron Microscope Facility, all as previously described.¹⁶ⁱ

addition, they provide a clean system for additional product, kinetic and mechanistic studies for a mode of decomposition in which a full, proved mass balance can in principle at least be obtained, a complete stoichiometry that is difficult to impossible to obtain quantitatively (and sometimes even qualitatively) for analogous solid-oxide-supported systems. (Preliminary, separate thermolysis studies of both of the $\text{M}(\text{CO})_2^+$ ($\text{M} = \text{Ir}, \text{Rh}$) compounds **2a** and **3** show that $\text{M}(0)$ metal apparently seen previously^{13f} for partially decomposed samples of **3** is *not* produced upon thermolysis of a 30 mM solution in CH_3CN for 48 h under nitrogen at 60 °C.)

Formation of Rh_n^0 Nanoclusters from $[\text{Rh}(\text{CO})_2\cdot\text{P}_2\text{W}_{15}\text{Nb}_3\text{O}_{62}]^{8-}$ Under H_2 and Photolysis: Evidence for the Relationship of $[\text{M}(\text{CO})_2\cdot\text{P}_2\text{W}_{15}\text{Nb}_3\text{O}_{62}]^{8-}$ ($\text{M} = \text{Rh}, \text{Ir}$) to Solid-oxide-supported $\text{M}(\text{CO})_2\cdot\text{Al}_2\text{O}_3$. Worth noting here is our preliminary work in 1987 with less well characterized “ $[\text{Rh}(\text{CO})_2\cdot\text{P}_2\text{W}_{15}\text{Nb}_3\text{O}_{62}]^{8-}$ ” made at room temperature. In solution, when irradiated in the presence of hydrogen and cyclohexene, an active hydrogenation catalyst is formed, one that even our 1987 ultracentrifugation molecular weight and other evidence indicated was a Rh_n^0 “colloid”.^{13f} We now know that a novel polyoxoanion-stabilized^{16i, 27} Rh_n^0 nanocluster is formed.¹³ⁱ We repeated this key experiment as part of the present work (see the details provided in the Experimental Section), and again observe the formation of black, isolable and acetone-soluble precipitate, after the hydrogenation of cyclohexene is complete. A TEM (transmission electron microscopy) study of this material verifies that ca. 10 to 40 Å nanoclusters have been formed, Figure 12.

The significance of these results is in their very strong analogy to Yates’ work studying atomically-dispersed $\text{Rh}(\text{CO})_2^+$ on solid Al_2O_3 .^{10e} In this analogous work, Yates and co-workers observe that $\text{Rh}(\text{CO})_2^+\cdot\text{Al}_2\text{O}_3$ loses a CO upon photolysis and that the resultant $\text{Rh}(\text{CO})_1^+\cdot\text{Al}_2\text{O}_3$ is reduced under H_2 to form $\text{Rh}(0)$,

which in turn yields Rh^0_n clusters on Al_2O_3 —a process that, intriguingly, is largely reversible if CO is readded.^{2b,4,8,10}

As is perhaps obvious, the formation of a black, active Rh^0_n nanocluster catalyst herein from the $[\text{Rh}(\text{CO})_2 \cdot \text{P}_2\text{W}_{15}\text{Nb}_3\text{O}_{62}]^{8-}$ precursor is, at least presently and phenomenologically, one of the best examples available of the very close resemblance between the *reaction chemistry* of a solid metal-oxide-supported monometallic carbonyl and polyoxoanion-supported $\text{M}(\text{CO})_n^+$.

Summary

(1) The polyoxoanion-supported, C_{3v} symmetry $\text{Re}(\text{CO})_3^+$ complex, $[\text{Re}(\text{CO})_3 \cdot \text{P}_2\text{W}_{15}\text{Nb}_3\text{O}_{62}]^{8-}$, has been synthesized and characterized in two different countercation compositions. The $[(n\text{-C}_4\text{H}_9)_4\text{N}]_8^{8+}$ salt is a highly soluble, air-stable compound which exists as a single isomer in solution. The $[(n\text{-C}_4\text{H}_9)_4\text{N}]_5\text{Na}_3^{8+}$ salt provides a lower solubility, chemically pure product (*i.e.*, without contaminating $(n\text{-C}_4\text{H}_9)_4\text{NBF}_4$), which also exists as a single isomer in solution (following treatment with Kryptofix[2.2.2] and brief heating to remove Na^+ ion-pairing effects).

(2) The polyoxoanion-supported $\text{Ir}(\text{CO})_2^+$ complex $[\text{Ir}(\text{CO})_2 \cdot \text{P}_2\text{W}_{15}\text{Nb}_3\text{O}_{62}]^{8-}$ has been synthesized and characterized as its $[(n\text{-C}_4\text{H}_9)_4\text{N}]_8^{8+}$ salt. The ^{31}P NMR and IR spectra show that this complex also exists as a single isomer in solution. This complex is found to be air- and water-sensitive.

(3) Attempted preparation of the analogous $\text{P}_2\text{W}_{15}\text{Nb}_3\text{O}_{62}^{9-}$ -supported $\text{Rh}(\text{CO})_2^+$ complex has revealed that this compound is unstable in solution at room temperature. Even low-temperature isolation yields a material that is 20% decomposed.

(4) Work with the Na^+ -containing salts of both the supported $\text{Re}(\text{CO})_3^+$, **1b**, and the $\text{Ir}(\text{CO})_2^+$, **2b**, complexes has revealed that two isomers (one C_{3v} and one non- C_{3v} symmetry) are present for each of these complexes. As such, they (or, possibly better, their mono- Na^+ salts) are identified as key systems for further structural,²⁵ kinetic, mechanistic and ΔH^\ddagger and ΔS^\ddagger activation parameter studies of metal cation, $\text{M}(\text{CO})_m^+$ mobility on an oxide surface.

(5) The three $[\text{M}(\text{CO})_n \cdot \text{P}_2\text{W}_{15}\text{Nb}_3\text{O}_{62}]^{8-}$ ($\text{M} = \text{Re}, \text{Ir}, \text{Rh}$) systems reported herein have been identified as useful ones for product, kinetic, and mechanistic studies of the mode(s) of decomposition of $\text{M}(\text{CO})_n^+$ on oxides, a topic of interest since such metal carbonyls are used as precursors to heterogeneous catalysts.

(6) The photochemical activation under H_2 of the $\text{Rh}(\text{CO})_2^+$ complex **3** has been demonstrated, results which (a) provide a new route to novel polyoxoanion-stabilized nanoclusters^{16l,27}

(27) A Perspective on Nanocluster Catalysis: Polyoxoanion and $(n\text{-C}_4\text{H}_9)_4\text{N}^+$ Stabilized $\text{Ir}(0)_{\sim 300}$ Nanocluster “Soluble Heterogeneous Catalysts.” Aiken, J. D., III; Lin, Y.; Finke, R. G. *J. Mol. Catal.* **1996**, *114*, 29.

(*i.e.*, from $[\text{M}(\text{CO})_n \cdot \text{P}_2\text{W}_{15}\text{Nb}_3\text{O}_{62}]^{8-}$ precursors) and (b) establish one of the best connections to date between the reaction chemistry of a *polyoxoanion-supported* and a *solid-oxide-supported* organometallic.

(7) Finally, the present three $[\text{M}(\text{CO})_n \cdot \text{P}_2\text{W}_{15}\text{Nb}_3\text{O}_{62}]^{8-}$ complexes provide 1-to-1 metal-to-soluble oxide, unaggregated, and single isomer ($\text{M} = \text{Re}, \text{Ir}$), model complexes for needed EXAFS and other spectroscopic studies of solid-oxide-supported $\text{M}(\text{CO})_n^+$ ($\text{M} = \text{Re}, \text{Ir}, \text{Rh}$). Their only—but main—disadvantage is that such 8− salts of Dawson-type polyoxoanions have not proven crystalline (*i.e.*, for X-ray diffraction structures) despite considerable efforts toward this goal (see the Supplementary Material elsewhere^{16j}).

In closing, we note that only conclusions 1, 2, 5, and 7 were among our initial goals when this work was initiated more than a decade ago.^{13f} The present studies illustrate a few of the hidden, additional findings (*i.e.*, points 3, 4, and 6 above) available in polyoxoanion soluble metal oxides, but also the time and effort required to uncover them.

Acknowledgment. We thank Dr. Brian Arbogast of Oregon State University for FAB-MS measurements, Dr. Eric Schabtach at the University of Oregon Electron Microscope Facility for the TEM shown in Figure 12, and Dr. Christopher Rithner of Colorado State University for ^{183}W -NMR measurements. This work was supported by the Department of Energy, Chemical Sciences Division, Office of Basic Energy, via Grant DOE-FG06-089ER13998 and, more recently, by NSF Grant No. CHE-9531110. T.N. thanks the Japan Society for the Promotion of Science for postdoctoral fellowship. H.W. thanks the German Academic Exchange Service, DAAD, Bonn, Germany, for a postdoctoral fellowship.

Supporting Information Available: Table of CO stretching wavenumbers for various $\text{M}(\text{CO})_n^+$ compounds (Table A), text giving the calibration procedure for the gas-uptake line, and figure showing the apparatus for reaction with carbon monoxide (Figure A), gas-uptake apparatus (Figure B), positive FAB-MS spectrum of $[(n\text{-C}_4\text{H}_9)_4\text{N}]_8[\text{Re}(\text{CO})_3 \cdot \text{P}_2\text{W}_{15}\text{Nb}_3\text{O}_{62}] \cdot (n\text{-C}_4\text{H}_9)_4\text{NBF}_4$, **1a** (Figure C), ^1H NMR of $[(n\text{-C}_4\text{H}_9)_4\text{N}]_5\text{Na}_3[\text{Re}(\text{CO})_3 \cdot \text{P}_2\text{W}_{15}\text{Nb}_3\text{O}_{62}]$, **1b**, with 3 equiv of Kryptofix[2.2.2] (Figure D), ^{183}W NMR of **1b** (Figure E), ^{19}F NMR of **1b**, after multiple reprecipitations (Figure F), time-dependent change of ^{31}P NMR of $[(n\text{-C}_4\text{H}_9)_4\text{N}]_8[\text{Ir}(\text{CO})_2 \cdot \text{P}_2\text{W}_{15}\text{Nb}_3\text{O}_{62}] \cdot (n\text{-C}_4\text{H}_9)_4\text{NBF}_4$, **2a**, in CD_3CN (Figure G), change of ^{31}P NMR of **2a** in the presence of H_2O (Figure H); change of ^{31}P NMR of **2a** after exposure to air (Figure I), ^{31}P NMR of **2a**, with subsequent addition of 3 equiv of NaBF_4 and 3 equiv of Kryptofix in CD_3CN (Figure J), IR spectrum of **3** (Figure K), and the time-dependent change in the ^{31}P NMR of $[(n\text{-C}_4\text{H}_9)_4\text{N}]_8[\text{Rh}(\text{CO})_2 \cdot \text{P}_2\text{W}_{15}\text{Nb}_3\text{O}_{62}] \cdot (n\text{-C}_4\text{H}_9)_4\text{NBF}_4$, **3**, in CD_2Cl_2 (Figure L) and in CD_3CN (Figure M) (16 pages). Ordering information is given on any masthead page.

IC960910A